POLITECNICO DI TORINO

Corso di Laurea Magistrale in “Mechanical Engineering”

Master’s thesis

Steady-state turbogas plant performance optimisation through mean-line and stream-line analysis of turbine and compressor

RELATORI:

Prof.ssa Daniela Misul
Prof. Mirko Baratta

CANDIDATO:

Simone D’Imperio

TUTOR AZIENDALI:

Ing. Luca Forno
Ing. Marco Toppino

Anno Accademico 2018/2019

A mia madre Rita, mio fratello Ilario

ed alla memoria di mio padre Mimmo

Index

Abstract

This thesis project takes place in the context of heavy-duty gas turbines production, evolution and upgrades. Given the trends going more and more towards higher output powers in order to satisfy the energy demand, increased efficiencies and lower emissions to deal with the stringent regulations imposed by the Countries concerning environment on the one hand and the necessity to guarantee a machine life as long as possible to amortise its capital cost on the other one, the partial re-design of old generation machines to make them competitive on the market with new generation ones becomes predominant.
The focus of the present thesis is centred on an engine, the FIAT TG20 B7/8, whose original design dates back to the Seventies, moreover many turbo-gas plants all over the world still present this machine.
The main objective has been to carry out an analysis of the machine able to pave the way for all the modifications necessary to increase power and efficiency.
The most important parameters (turbine inlet temperature and cooling mass flow rate) to act on have been identified according to the possibility of performing simple and low-cost yet effective and well-studied changes. The critical issues generated from these modifications have been taken in account and dealt with consistently.
The starting point of the present work has been a series of sensitivity analyses, conducted on the PH4145 software from a mean-line standpoint, in order to understand the general behaviour of the machine. Taken in account these initial analyses, the assessment has been to increase the turbine inlet temperature and to reduce the cooling air mass flow rate.
Even though this action may appear as a countersense, it must be specified that in the original design a not so high attention was paid to all the possible leakages which could come from the cooling circuit, therefore the idea behind that has been to reduce the cooling air mass flow rates where not needed, to reduce the leakages and to keep the necessary ones possibly unchanged coherently to the mechanical part creep resistance and admitted deformations linked to the new turbine inlet temperature.
Consequently, the cooling system has been deeply analysed on the software PH4165, in order to find the critical spots and strategies able to reach the above-mentioned target, still applying slight modifications on the mechanical parts, which do not represent a problem from the manufacturing, mounting or cost point of view.
The last part has consisted instead in a sort of validation of all the work previously done, in fact the same machine has been studied by using two completely different softwares. One of them (PH4145), which dates back to the Seventies as well, is able to perform the analysis just from a mean-line standpoint and all the characteristics of the machine have to be input manually, starting from drawings. The other one (AxSTREAM), a more modern software, is able to perform both a mean-line and a stream-line analysis where the geometry of the machine can be directly acquired from 3-D CAD models. The stream-line approach becomes then important for the thermo-structural validation of the work, as it supplies the boundary conditions, and to put in evidence some criticalities of the modifications the machine should undergo.
The two softwares have been compared from a mean-line point of view, leading to outputs which deviate by a small, constant amount, considering different turbine inlet temperatures and cooling conditions.
All the considerations and analyses made in this work, may then lead to a relatively new machine, able to compete with new generations ones.

1. Energy outlook: development and production

This chapter is meant to introduce the reader to the importance that energy has always had in the universe history, how it has been dealt with by humans and exploited at its best as well as to give him/her the fundamental thermodynamic knowledge on one of the methodologies through which it can be produced, namely the Joule-Brayton cycle, since it represents the basis of all the considerations and developments done in this work.

1.1 History and environment

"Energy is defined as the capacity of a system to perform work".
"Everything is energy".

Whether it is observed from a "classical" or a more "modern" standpoint, the importance of its role in universe especially regarding earth and humankind development is undoubtedly tangible.
Energy allowed life on this planet through the oldest source that could be thought about, the sun. It has been providing light and heat for millions of years, thus generating a series of interconnected events (photosynthesis, rain, wind) which together contribute to this fascinating and mysterious existence.
Even though it could be considered as an endless power source on the relatively short run, humans at their early stage had to think of other means to exploit it, due to the impossibility of managing and controlling the solar one.
The first alternative explored was the wood, by burning it, it was possible to obtain warmth, light and cooked food. Later on, it has started involving other activities, such as metals production.
As time was passing by, human dependence on energy became stronger and stronger because of an increase in population and shortage of wood, therefore the need of other sources became relevant.
The first industrial revolution completely changed the focus, steam engines were built and fossil fuels adopted; it became a competition in which faster, bigger machines represented a hopeful technological advance.
Up to now, due to the continuous primary energy demand increase, different technologies suited for energy production have been developed, thus involving various sources (wind, solar, natural gas, oil, coal, nuclear, hydropower) in function of the need and possibility of exploiting them.

Figure 1.1.1 [1] shows the global primary energy consumption across the last two centuries as far as 2017 in quantitative terms and a produced energy distribution according to the different sources that are actually used.

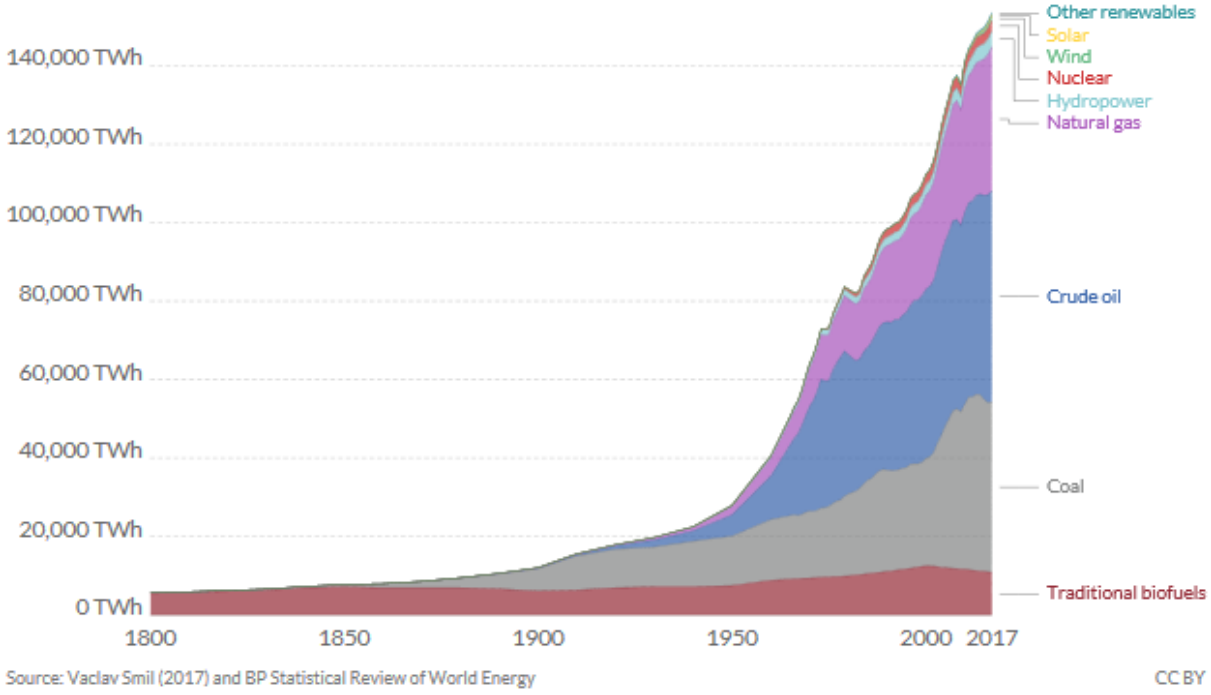

Figure 1.1.1 – Global primary energy consumption.

As it can be noticed, the major energy supply percentage directly arises from fossil fuels, therefore combustion mechanisms are involved with an important drawback: the impact of these reactions is not negligible if human health and environment are considered.
Among combustion products, it is possible to find:

- CO_2, greenhouse gas responsible for earth overheating;
- CO, toxic molecule, which indissolubly links to blood red cells;
- HC, carcinogenic molecules;
- NO_x, irritating for mucouses.

All these polluting agents are defined as “primary”, since there is the possibility that some of them may react with each other leading to other polluting substances (for instance photochemical smog).
Living organisms were not “designed” to deal with this kind of external agents, at least not in an exaggerated amount and the effects on health caused by them is more than real.
One thing more to consider is that earth operates on a very delicate equilibrium, slight changes of the boundary conditions may lead to catastrophic consequences (just thinking about the fact that a global increase in temperature of few degrees could induce hurricanes, tornadoes and floods).
Furthermore, fossil fuel supplies are quickly being used up, its cost varies according to market trends so the need of alternative or more efficient technologies is becoming more and more predominant.

Some conclusions can therefore be drawn. On the one hand energy demand is increasing and the existing technologies are more than able to satisfy it, on the other one the risks are enormous; in addition to this, many plants for high power generation represent a huge capital cost for a firm interested in dealing energy.

In this delicate and complex context, the object of the present thesis may be included, in particular, focusing the attention just on the electrical power generation by means of turbo-gas plants the main requirements consist in modifications able to guarantee:

- higher output power;
- increased efficiency;
- low pollutant emissions (NO_x is the critical issue, since the combustion happens in lean charge).

Over the years a strong evolution has been carried out (nowadays plants are defined as 5^{th} generation) working on various aspects.
The easiest and most important one is the increase of the turbine inlet temperature able to guarantee a higher output power and an increased efficiency, which has led to the development and of more resistant materials (creep, centrifugal stresses, thermal stresses).
The compression ratio has been increased according to the admitted structural limitations and a more careful study of the combustion process has been assessed.

1.2 Electrical energy production, Joule-Brayton cycle

As previously mentioned, one of the ways through which electrical energy can be obtained is through a turbo-gas plant.
The plant, schematically represented on the left part of Figure 1.2.1, is essentially composed of:

- a compressor, needed to increase the pressure of the working fluid (air);
- a burner, in which lean combustion takes place;
- a turbine which is kept in rotation by the gas high temperature and pressure by expanding the latter and carrying the compressor and a generator on the same shaft;
- a generator, which is able to transform the rotational movement of the rotor into electrical energy according to the Faraday effect.

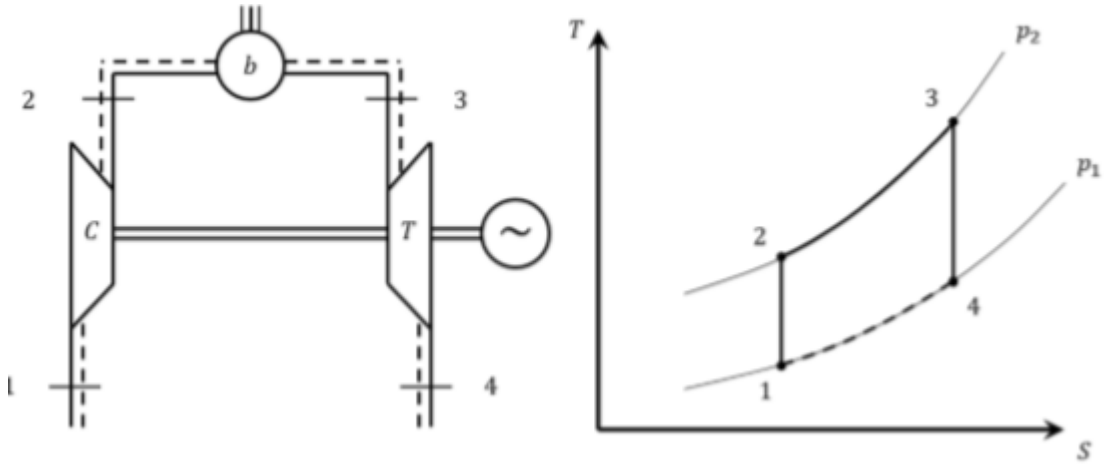

Figure 1.2.1 – Turbo gas sketch and ideal Joule-Brayton cycle.

From a thermodynamic point of view the fluid performs a Joule-Brayton cycle, which represents the ideal reference, composed of four transformations, which are:

- *1-2*, working fluid adiabatic compression;
- *2-3*, working fluid constant pressure heating (models the combustion);
- *3-4*, working fluid adiabatic expansion
- *4-1*, working fluid cooling, represented by a dashed line since the cycle is actually open.

In order to have a better insight on the performances of the turbo-gas plants, it may be useful to rely on the real cycle characterized by the fact that:

- dissociation takes place in the burner (higher sensibility over 1800 K);
- the compressor increases the pressure of air (c_p, R), the turbine expands burned gasses (c_p', R') characterised by a higher specific heat capacity and gas constant;
- viscous losses take place during the compression and expansion phases;
- the fluid experiences pressure losses through the plant devices.
- part of the compressed air is used in order to provide the adequate cooling in the turbine.

In the end, the ideal cycle gets modified as shown in Figure 1.2.2.

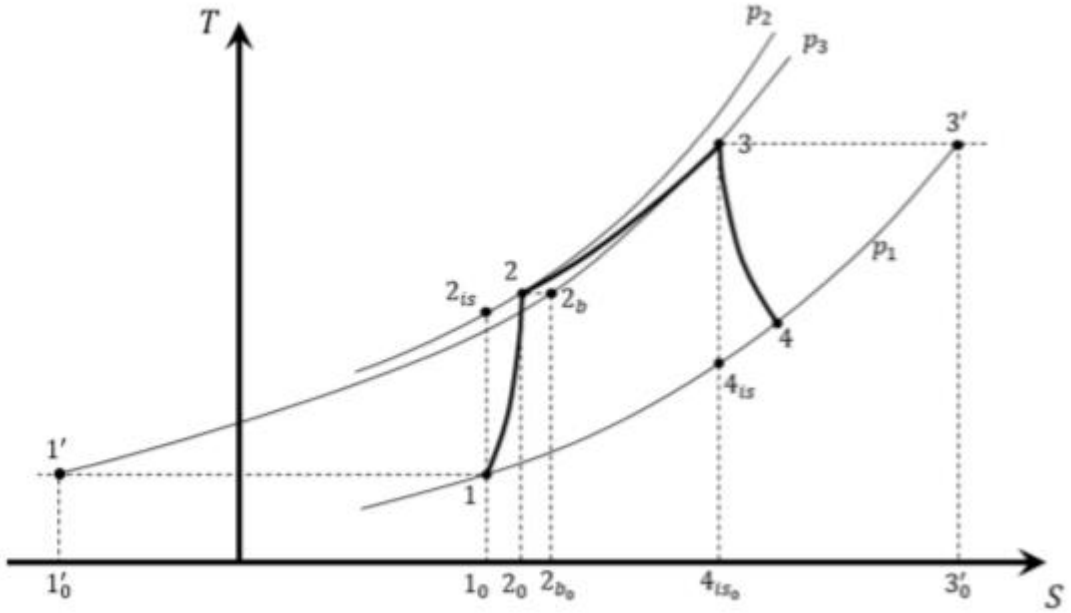

Figure 1.2.2 – Real Joule-Brayton cycle.

The power requested by the compressor is defined as:

$$P_c = \frac{1}{\eta_{is,c}} \dot{m}_a \, c_p T_1 (\beta_c^{\frac{k-1}{k}} - 1) \tag{1.2.1}$$

where:

- $\dot{m}_a$ is the air mass flow rate;
- $\eta_{is,c}$ is the isentropic efficiency of the compressor;
- T_1 is the air inlet temperature, compressor side;
- β_c is the compression ratio;
- k is the air adiabatic index.

The thermal power coming from the combustion is equal to:

$$\dot{Q}_1 = (\dot{m}_{a,cool} + \dot{m}_f) c'_p (T_3 - T_2) = \eta_b \, \dot{m}_f \, H_{LV} \tag{1.2.2}$$

where:

- $\dot{m}_f$ is the fuel mass flow rate;
- T_3 is the fluid temperature at the burner outlet, which is coincident to the turbine inlet;
- T_2 is the fluid temperature at the burner inlet, which is coincident to the compressor outlet;
- η_b is the burner efficiency;
- H_{LV} is the lower heating value of the fuel.

The power generated by the turbine is equal to:

$$P_t = \eta_{is,t}(\dot{m}_a + \dot{m}_f)c'_p T_3\left(1 - \frac{1}{\beta_t^{\frac{k'-1}{k'}}}\right) = \eta_{is,t}\,\dot{m}_a \frac{1+\alpha}{\alpha} c'_p T_3\left(1 - \frac{1}{\beta_t^{\frac{k'-1}{k'}}}\right) \tag{1.2.3}$$

where:

- $\eta_{is,t}$ is the turbine isentropic efficiency;
- β_t is the turbine expansion ratio;
- k' is the combustion products adiabatic index;
- α is the air to fuel ratio.

The wasted thermal power, due to the high temperature of the exhaust gasses is:

$$\dot{Q}_2 = (\dot{m}_a + \dot{m}_f)c'_p(T_4 - T_1) \tag{1.2.4}$$

where:

- T_4 is the turbine outlet temperature.

Summing up, the useful power is equal to:

$$P_u = \eta_m(P_t - P_c) \tag{1.2.5}$$

and the global efficiency, introducing also the turbine and compressor efficiencies:

$$\eta_g = \eta_m \eta_b \frac{\eta_{mt}\eta_{is,t}\left[\frac{T_3}{T_1}\frac{1}{\beta_c^{\frac{k-1}{k}}}\frac{\left(\beta_c^{\frac{k-1}{k}} - 1\right)}{\left(\frac{\beta}{\eta_{\pi b}}\right)^{\frac{k-1}{k}} - 1} - \frac{1}{\eta_{mc}\eta_{mt}\eta_{is,t}\eta_{is,c}}\right]}{\frac{\frac{T_3}{T_1} - \left(\frac{\beta}{\eta_{\pi b}}\right)^{\frac{k-1}{k}}}{\left(\frac{\beta}{\eta_{\pi b}}\right)^{\frac{k-1}{k}} - 1} - \frac{1-\eta_{is,c}}{\eta_{is,c}}} \tag{1.2.6}$$

By plotting the global efficiency as a function of the compression ratio and the turbine inlet temperature:

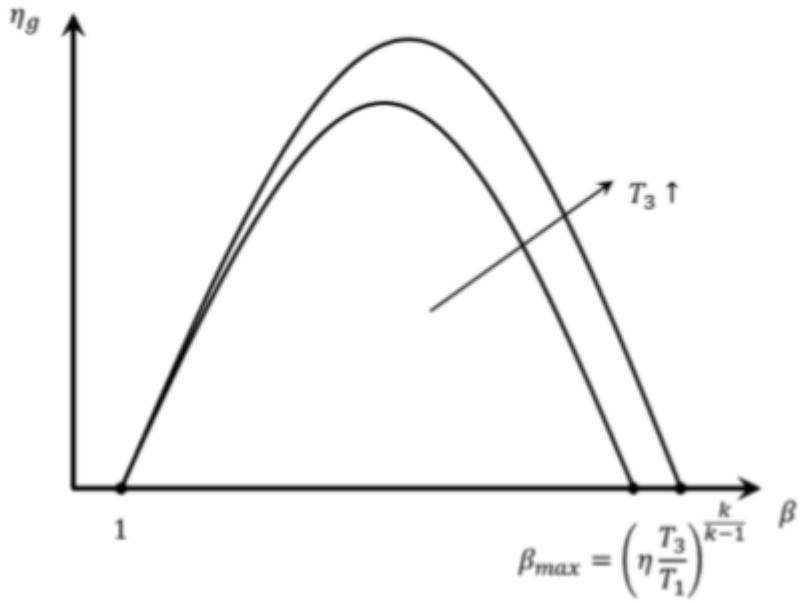

Figure 1.2.3 – Global efficiency trend.

It is evident how it increases by increasing the turbine inlet temperature and reaches a maximum value for a certain compression ratio. Since the maximum compression ratio shows a dependence on the turbine inlet temperature as well, as the temperature increases, the maximum of the curve shifts towards right [2].

1.3 Firm presentation: EthosEnergy Italia S.p.A

The realisation of the present thesis has been possible thanks to the collaboration between Polytechnic of Turin and EthosEnergy Italia S.p.A. The firm is specialised in gas turbines, with machine engineering services supplied by a team of expert technicians and engineers and a wide spare parts warehouse inventory.
It was founded in Turin in 1952 by Fiat group and started the gas turbine production with Westinghouse license contract, becoming a pillar in electrical power plants construction with 350 plants in 40 Countries. In 2000 the company became part of Siemens group changing the name first in Gas Turbine Technologies and then in TurboCare.
In 2014 EthosEnergy was created as joint venture between TurboCare, Siemens and Wood group in order to become an independent leader supplier in rotating machinery, services and solutions for energetic, gas & oil and industrial markets.
To the present day EthosEnergy Italia S.p.A is focused on core OEM and other OEM activities connected to the gas turbines construction and relative components production, parts repair, rotors overhauls, relocations and plants upgrades.
The italian plant has a wide production capacity and repair activity for different gas turbines technologies.
The firm is involved in:

- Core Engineering;
- Production Engineering;
- Application Engineering;
- Project Engineering.

The present work has been mostly carried out in the Core Engineering section, which is involved in:

- Machine parts design modifications;
- Design modification for cost reduction;
- Performances evaluation and monitoring.

2. TG20 B7/8, first design and upgrades over the years

The turbo-gas machine object of this work, the one on which a mean-line and a stream-line analysis have been carried out as it is shown later on, is the FIAT TG20 B7/8.
The machine original design was thought and brought to reality during the Seventies of the last century. Some might say that t is an old machine and it actually is, especially considering how fast technology for this kind of application has proceeded across the last fifty years, but there still is the interest, the willing and the need to study, modify and produce this machine. Why?

Firstly, the huge capital cost for a heavy-duty power generation must be considered. An investor is not able to extinguish it in a few years, therefore, since the aim is to get a profit by producing and consequently selling electricity, he/she has all the interest to make the machine work as long as possible, by focusing the attention on the critical issues and respecting all the programmed overhauls. The same consideration stands for the manufacturer, who is more than concerned to have a satisfied client. For this reason, a symbiotic process triggers, paving the way to all the possible low cost and well-studied modifications able to guarantee a longer life and better performances of the machine.
Second of all, the human approach towards the production has completely changed over the years. There is more awareness and attention for what concerns the environment and the performances of the machine. The former is mostly due to the relatively severe regulations which are imposed by the Countries in order not to exceed the established limits of polluting agents. The latter instead is linked to the fact that energy demand is continuously increasing over the years, thus creating the need to generate both a higher amount of power and consequently to reduce the wasted one to get a doubled gain. In addition to this, measuring instruments and techniques have been upgraded, leading to a better knowledge of all the interest parameters of the machine, characterised by more precise and accurate outputs.

In this context the evolution and development of the TG20 B7/8 can be inserted. Many have been the modifications this machine has been subjected to. Some of them thought to increase the performances, some others to solve problems linked to its functioning.

In the following pages, firstly a general presentation of the machine is provided, then a concise description of all the upgrades made during the years involving causes and solutions is presented [3].
Moreover, the starting configuration of the machine that has been necessary to develop all the consideration is presented, stressing the attention on the cooling system which will has been one of the most important focuses.

2.1 TG20 B7/8 design and working scheme

The original sketch of the machine can be appreciated in Figure 2.1.1.

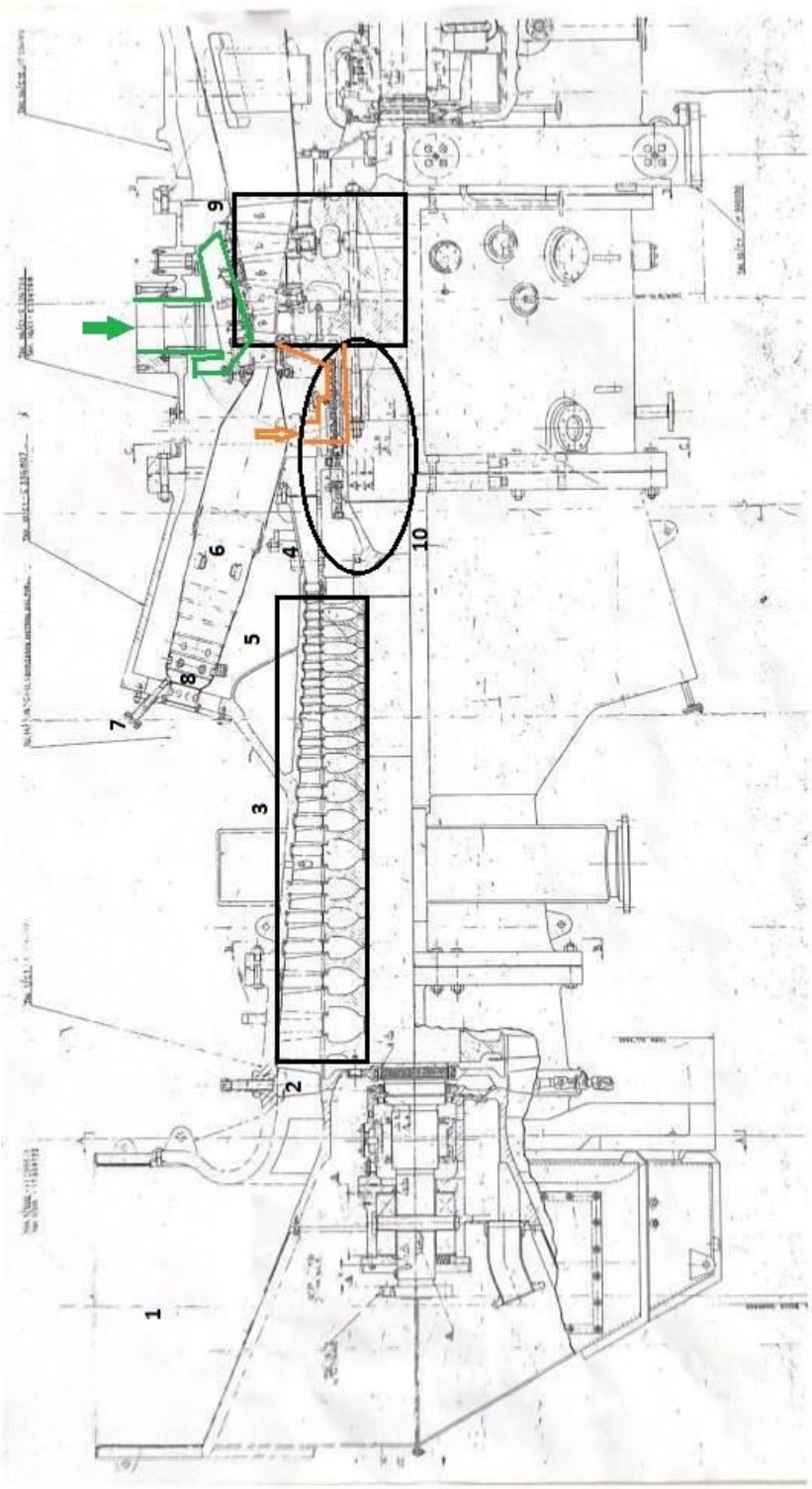

Figure 2.1.1 – Machine sketch.

The air is sucked by the compressor and firstly enters the inlet volute (1), passing then through the inlet guide vane (2) and consequently getting gradually compressed in the eighteen stages of the compressor (3) splined on a shaft connected to the turbine group (9). It is interesting to note a peculiarity of the Westinghouse technology and design, precisely the fact that the turbine group is not splined on a shaft, but connected to the compressor through the main flange and connecting bolts (10), the turbine rotors are kept together and compacted by means of eight steel tie rods.

By the way, once the air is compressed, after the diffuser (4) it enters the compressor delivery (5) and the burner (6) which by means of an injector (7) that allows the mixing with the fuel and a spark plug (8), makes the chemical reaction possible, generating in this way a remarkable increase in the enthalpy level. On the burner, holes perpendicular to machine londitudinal axis are present in order to reach the desired air to fuel ratio, thus preventing the turbine blades from being invested by the flame and reaching the desired turbine inlet temperature.

Once the air and fuel lean mixture enters the turbine group, it is expanded along the three stages. Its temperature and pressure gradually decrease generating work or equivalently mechanical power used to drag both the compressor and the electrical generator, not visible in the drawing.

The attention must be paid on the secondary flow as well, which is the cooling flow. No inter-stage bleeding in the compressor is present, which means that the air is completely bled at the compressor delivery. Afterward it is sent to an external cooler (not visible on the sketch) through a slot realised on the machine shell. This aspect represents a weakness of the machine since the total amount of cooling air is firstly compressed at its maximum leading also to a consequent increase in temperature where it is not needed since lower pressure and temperature values may be sufficient to cool the second and third stages. Of course, this represents a waste of work the compressor has to carry out anyway.

After the air is cooled in a heat exchanger, the cooling flow is split into two secondary flows. One is the responsible for the cooling of the statoric parts of the machine and is hence defined as “stator cooling” (green), whilst the second one is responsible for the cooling in the rotoric parts of the machine, therefore defined as “rotor cooling” (orange).

To be absolutely precise, this subdivision is a bit loose and the peculiarities will be clearer later on, but it still is sufficient to get the idea behind the approach towards cooling in this case.

In Table 2.1.1 the most important parameters of the machine are presented: power, efficiency, turbine inlet temperature, turbine inlet pressure, air mass flow rate and bled air necessary for cooling and so on.

Table 2.1.1 – Machine parameters, standard configuration.

Parameter	Value	Unit of measure
P_gen	37.8	[MW]
η_g	29.5	[%]
$T1T$	1353	[K]
T_{exh}	793	[K]
$T2C$	626.1	[K]
$P1T$	11.9	[bar]
$\dot{m}_a$	158.9	[kg/s]
$\dot{m}_{a,cool}$	16.3	[kg/s]
$\dot{m}_f$	3.1	[kg/s]
n	4918	[rpm]

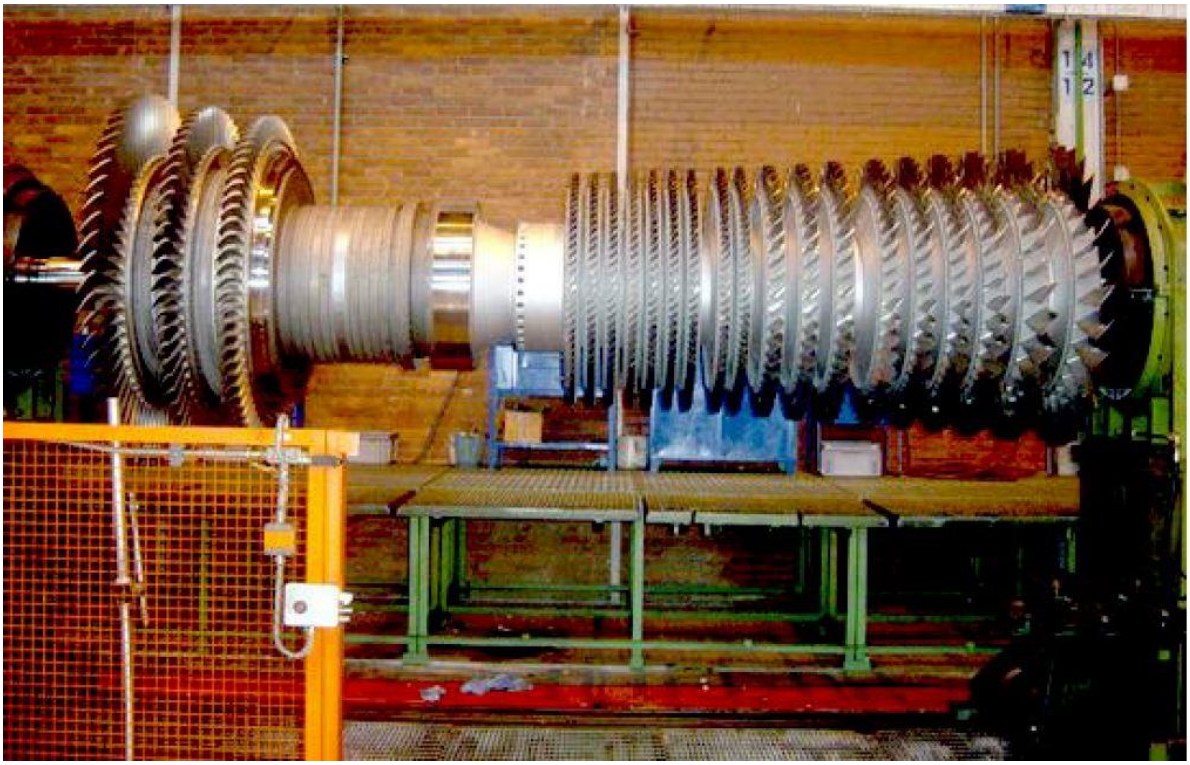

Figure 2.1.2 – TG20 B7/8 rotor.

2.2 TG20 B7/8 U

This is one of the modifications that the machine has undergone. The reason for it was mainly to increase the air mass flow rate at the compressor inlet, thus obtaining an increase in the output power. Together with that, an experimental study concerning the compressor conducted in the late Eighties evidenced high Mach numbers, high loads and high losses on the first stages of the compressor.
The conclusion was a partial redesign of the compressor stages. In particular, the parts interested by this upgrade were:

- Compressor inlet casing;
- Inlet Guide Vane (IGV);
- the first two rows of the compressor stationary blades;
- the first two rows of the compressor rotating blades.

By a proper design and a substitution of the above-mentioned parts the compressor inlet air flow increased by 3 % and a better compressor efficiency was obtained.

Table 2.2.1 – Machine parameters, U configuration.

Parameter	Value	Unit of measure
P_gen	39.7	[MW]
η_g	29.9	[%]
$T1T$	1353	[K]
T_{exh}	789	[K]
$T2C$	627.9	[K]
$P1T$	12.2	[bar]
$\dot{m}_a$	163.5	[kg/s]
$\dot{m}_{a,cool}$	17.4	[kg/s]
$\dot{m}_f$	3.2	[kg/s]
n	4918	[rpm]

2.3 TG20 B7/8 G

The need for this modification emerged after a Hot Part Inspection of some power plants, in which the examination highlighted a deformation of the inner shroud of a certain number of vane segments of the first stage which caused an interference between the statoric part and the rotating one, leading to severe consequences.
The analysis of the vanes, aimed at the cooling channels, made it clear that some of them were clogged by fine dust particles (problem particularly felt in dusty/sandy places) thus closing the channel and leading to an overheating of the considered part.
The solution to this problem consisted in a new arrangement of the cooling circuit, adopting the conceptual scheme of more recent machines.
To be precise, in the "G" configuration the first vane is directly fed by the combustor shell to guarantee a higher pressurisation and consequently allow a higher cooling holes cleanliness.
In Figure 2.3.1 the comparison between the standard and the "G" configuration is shown.

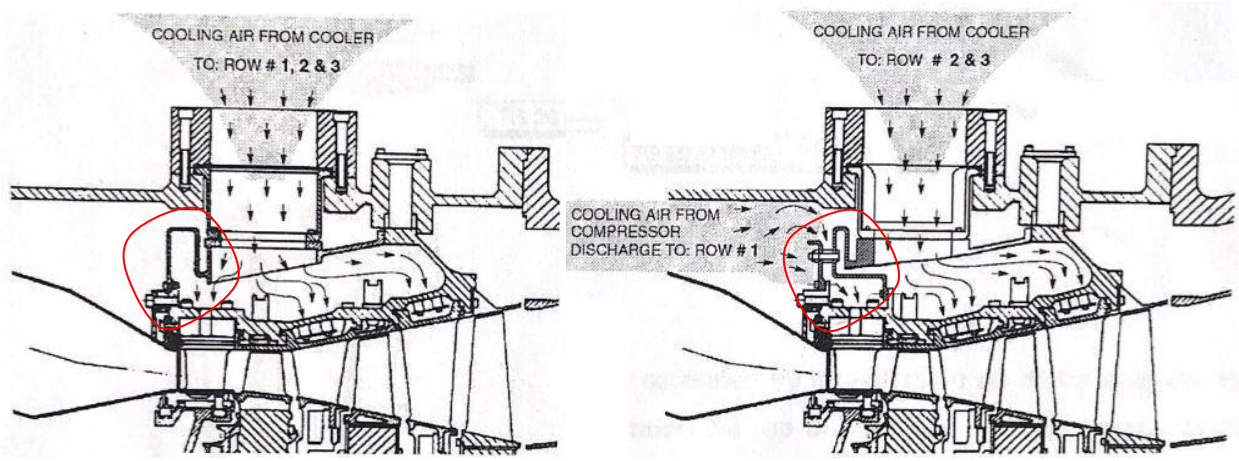

Figure 2.3.1 – Standard configuration (left) and "G" configuration (right).

Table 2.3.1 – Machine parameters, G configuration.

Parameter	Value	Unit of measure
P_gen	37.8	[MW]
η_g	29.5	[%]
$T1T$	1363	[K]
T_{exh}	793	[K]
$T2C$	626.2	[K]
$P1T$	11.9	[bar]
$\dot{m}_a$	158.9	[kg/s]
$\dot{m}_{a,cool}$	18.6	[kg/s]
$\dot{m}_f$	3.1	[kg/s]
n	4918	[rpm]

2.4 TG20 B7/8 mod.1

The need for this modification arose from the fact that some turbine disks, particularly in the second stage, failed due to an over-temperature of the latter.
The cooling for this component is realised by the stator cooling circuit. To be precise the air flowing in the second vane does not completely exit from the trailing edge, some of it is used in order to pressurise a chamber present under the vane. Given the pressure difference between this chamber and the second turbine disk, or equivalently the blade root, through properly designed holes an air flow is imposed from left to right (Figure 2.4.1).
The exact functioning of the disk may be compromised by any deviation present in the real machine from the ideal design (clearances during hot working, exact sealing assembly and so on).
Since it is not possible to exactly evaluate possible modification of the machine parts during steady-state condition, the solution consisted in an increase of the above-mentioned air flow rate in order to avoid gas ingestion phenomena without changing all the other cooling flows.
The modification consisted in increasing the holes diameter of:

- blade ring nozzles;
- seal ring;
- inlet plate;
- outlet plate.

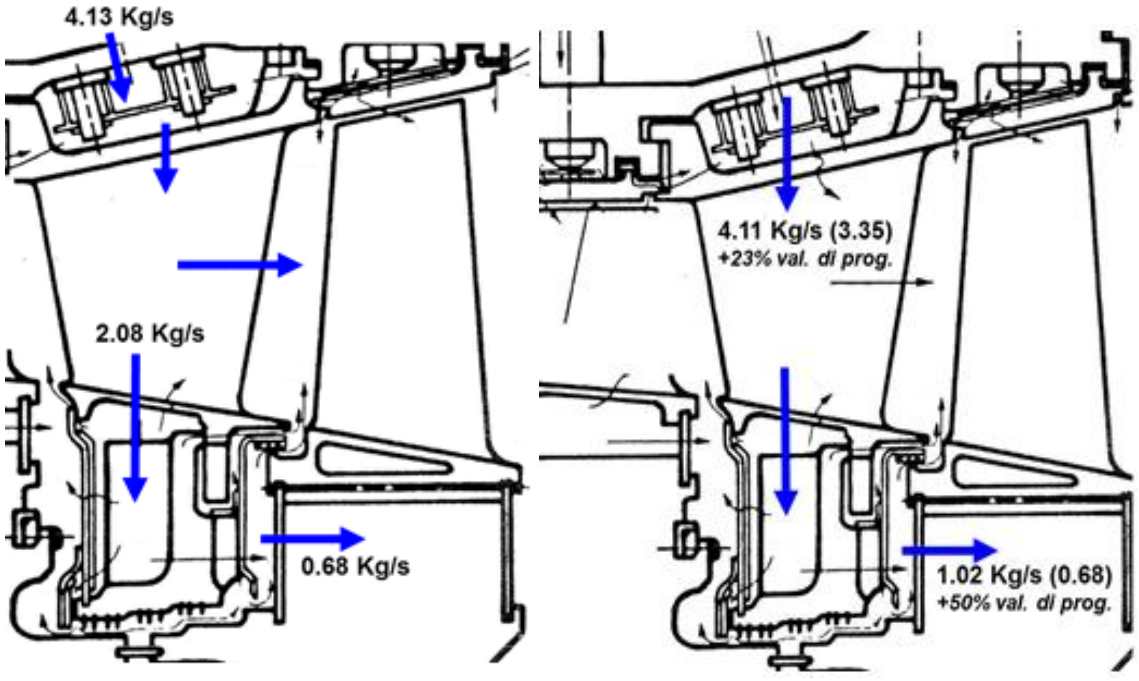

Figure 2.4.1 – Second vane air cooling schematic representation.
Standard configuration (left) and mod.1 configuration (right).

2.5 TG20 B7/8 mod.2

The mod.2 configuration was carried out in order to have a more modern, efficient and effective solution to the problem already presented in the Paragraph 2.4, by exploiting also the advantage to have cooling channels in the second blade. To be precise, the second disk is no more cooled by the stator cooling, but instead by the rotor cooling, therefore some modifications have been carried out in this direction.
The new design consisted in realising as many holes as the number of blades on the second disk, thus allowing a flow from the rotor cooling system to the second blade tip (Figure 2.5.1).

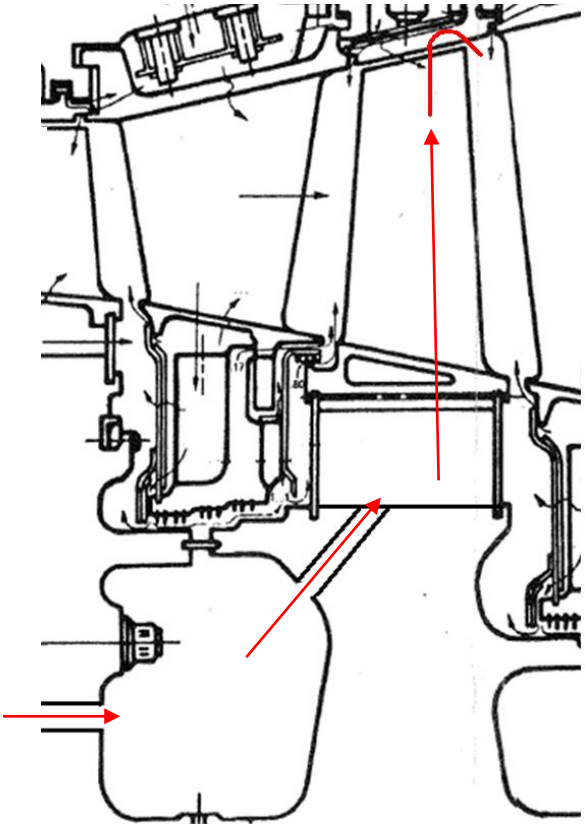

Figure 2.5.1 – Mod.2 configuration cooling arrangement.

2.6 TG20 B7/8 mod.3

This configuration represents the work of the present thesis. The attention is mainly focused on the three predominant aspects, which are useful power (measured at the generator), efficiency and NOx limits. The aim is to get an increase in the performances and a reduction in the polluting emissions. In Table 2.6.1 the goals are listed.

Table 2.6.1 – Mod.3 configuration targets.

Parameter	Value	Unit of measure
P_gen	45.4	[MW]
η_g	31.5	[%]
NOx	25	[ppm]

The mean-line analysis allows to study the machine from a one-dimensional point of view, taking in account how the changes of some boundary conditions, or better, some machine parameters of interest lead to certain outputs. It is a powerful tool that can be exploited on a first basis, in order to understand the macro-modifications that have to be followed according to the target one wants to reach, the feasibility of certain changes and the consistency to the theory. A certain number of sensitivity analyses have been carried out according to this approach.

The stream-line analysis instead allows to get a better insight on the machine, in particular on the flow path, leading to a better knowledge from a two-dimensional point of view. This can lead to understand all the critical points and to put the basis and boundary conditions for a thermo-structural analysis as well, from a more realistic and precise standpoint.

Furthermore, all the modifications will be applied to a particular configuration of the machine, precisely the "UG", which links together the "G" configuration and the "U" one. Therefore, this is the starting point. In Table 2.6.2 the parameters of interest are reported.

Table 2.6.2 – Machine parameters, UG configuration.

Parameter	Value	Unit of measure
P_gen	39.7	[MW]
η_g	29.9	[%]
$T1T$	1367	[K]
T_{exh}	790	[K]
$T2C$	628	[K]
$P1T$	11.7	[bar]
$\dot{m}_a$	163.5	[kg/s]
$\dot{m}_{a,cool}$	19.9	[kg/s]
$\dot{m}_f$	3.2	[kg/s]
n	4918	[rpm]

2.6.1 Stator cooling circuit

In this paragraph a description of the stator cooling is proposed. It is a cooling system realised in the internal part of the machine. Given its complexity, each part is presented separately from the others. In Figure 2.6.1.1 a schematic representation of the stator cooling is shown.

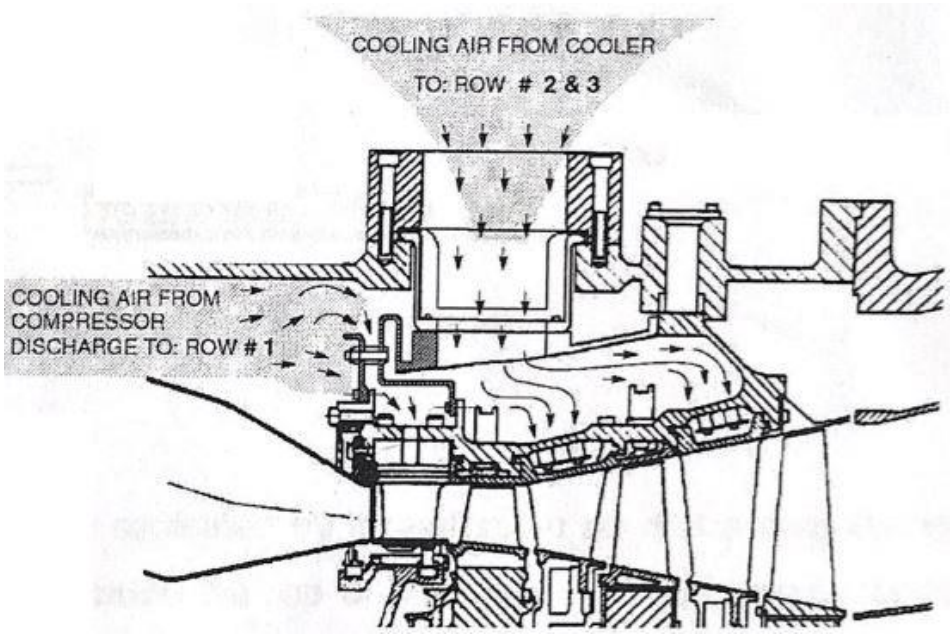

Figure 2.6.1.1 – Stator cooling.

As it can be noticed, the first vane of the turbine is directly fed by the compressor delivery as was dealt with in the "G" configuration. The second and third vane instead are fed by the air flow that has previously crossed the air cooler. The chamber realised between the external shell of the machine and the blade ring is kept under a high constant pressure level by the continuous air flow.
This aspect is necessary in order to guarantee the sufficient pressurisation level, the adequate cooling and to avoid gas ingestion phenomena, which, as previously said, could be very dangerous leading to an overtemperature and reducing the resistance of the material.
Starting from this general description, it is necessary to analyse each component connected to the cooling circuit.

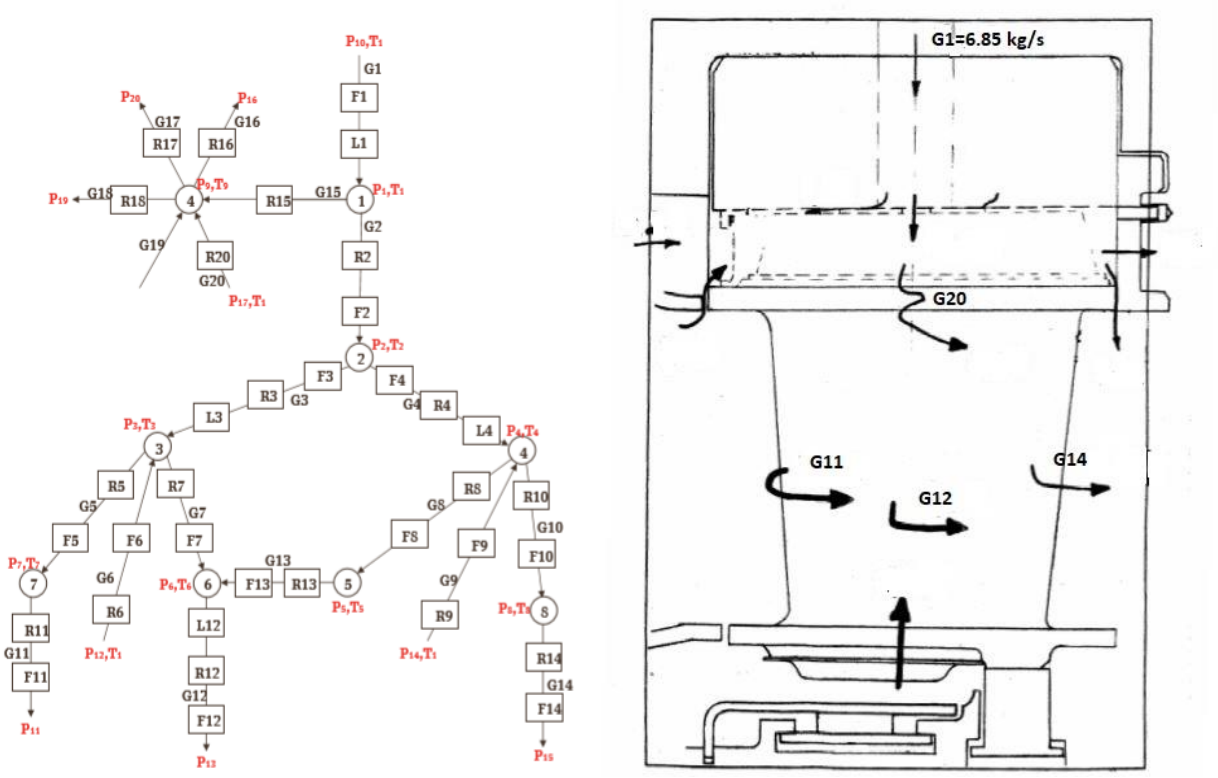

Figure 2.6.1.2 – First vane cooling schematic representation.

On the left part of Figure 2.6.1.2 the logical circuit that models the cooling circuit according to the used software (PH4165) is present. A precise description of the software modus operandi is presented in Paragraph 4.1.
It is interesting how these sketches were previously developed. Being the machine an old one as well as the in-house software PH4165, an accurate study on the real components was carried out years ago, recreating on the software all the restrictions and reasonably assuming possible turbulences or distributed and concentrated losses, according to theory. No 3 D model existed, most of the work was hand-made, but still the output of this software and models can easily compete with more modern ones.
As it can be appreciated, an initial air mass flow rate (G1) enters the vane through proper passages realised on it. Some leakages (indicated by the arrows in the sketch) along the axial diretion are present due to the non-exact coupling and small clearances that may be present in the machine. The air mass flow rates G11, G12 and G14 are instead the ones exiting the trailing edge, responsible for the vane cooling and mixing with the principal flux, whilst the mass flow rate G20 is a leakage flowing in the radial direction (that is why the curvy arrow).

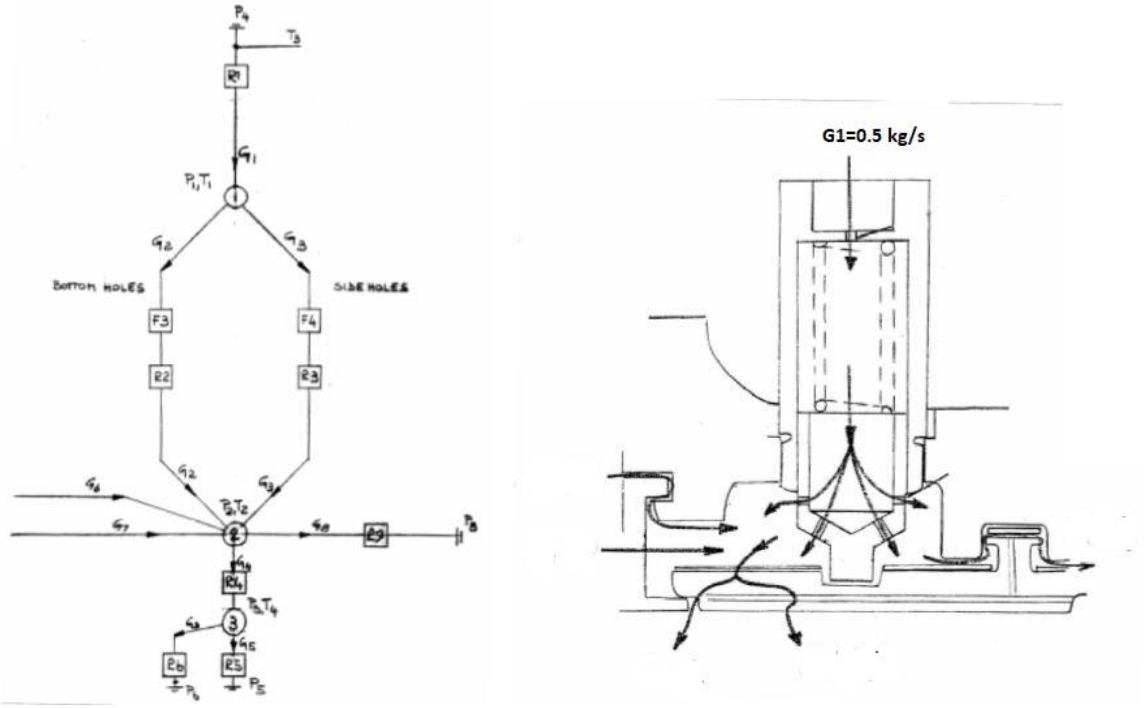

Figure 2.6.1.3 – Ring segment cooling schematic representation.

The ring segment is a plate present above the blade and between two vanes, its shape is such that the coupling between the vanes is guaranteed. Concerning its function, a small cooling air flow rate flows out from a nozzle realised on the blade ring and crosses the considered element. Afterwards part of it may flow through some mounting blacklashes which are always present, in particular, during hot functioning, the other part mixes with the principal flow in order to avoid gas ingestion phenomena, which can be more evident as the principal flow is centrifugated in the rotor.
As it can be noticed, a not so high air mass flow rate can be sufficient in order to perform the required function.

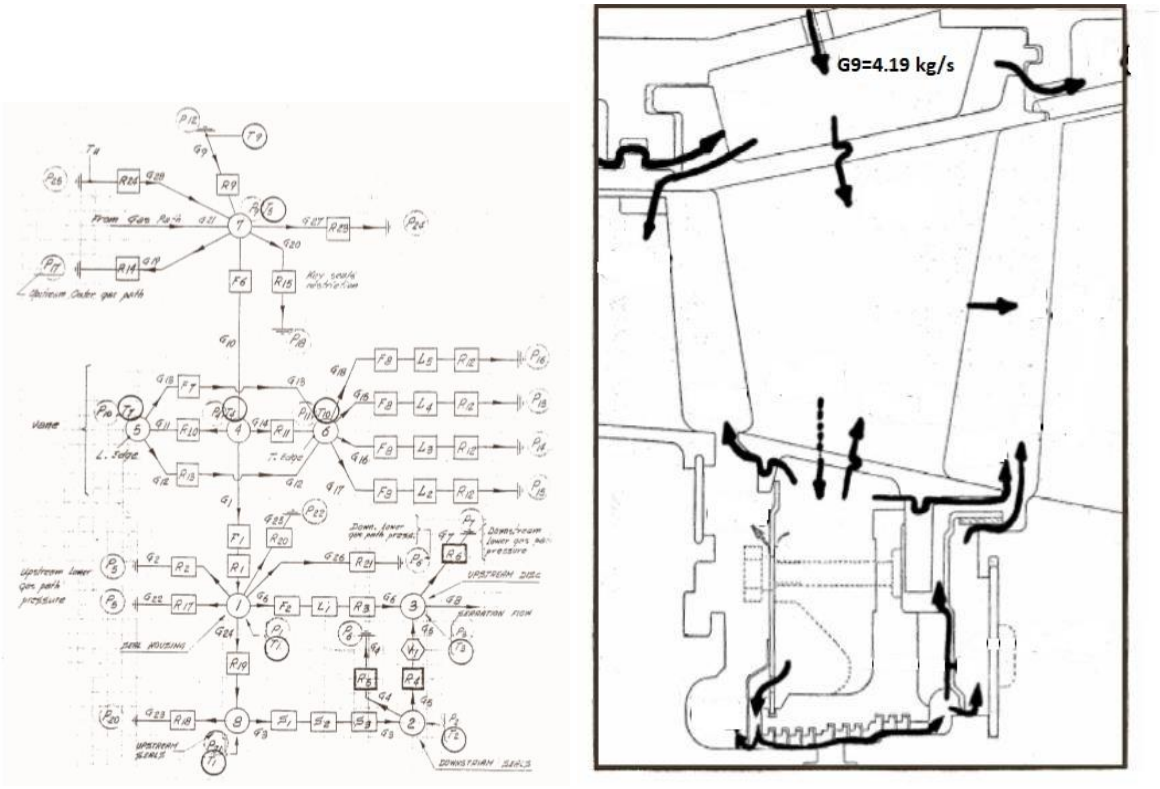

Figure 2.6.1.4 – Second vane cooling schematic representation.

The second vane is structurally different from the first one and so is the cooling flow network.
In particular, the air mass flow rate still enters the element from the upper part through a hole (G9) and leakages are present as well. The flow crosses the element and a certain flow rate exits the trailing edge as is valid for the first vane, but the main difference is in this case that a hole in the lower part of the vane is present. This allows to pressurise the chamber realised under it, bounded by steel circular crowns on the right and left side and by a labyrinth seal on the lower side, right above the two disks.
This configuration is definitely useful as it allows to contrast gas ingestion, thanks to the mass flow rates flowing between first disk and vane and second disk and vane but also because it was previously used in order to guarantee a mass flow rate necessary to cool the second row blade root.
In the mod.3 configuration of the machine this mass flow rate is suppressed as the second blade is directly cooled by the rotor cooling circuit.

Going on, the other main components schemes and pictures of the stator cooling circuit are reported, a description has not been made though, as the logic for second ring segment and third vane is exactly the same analysed for the previous ones, with the exception that in the third vane no cooling flow exits from the trailing edge.

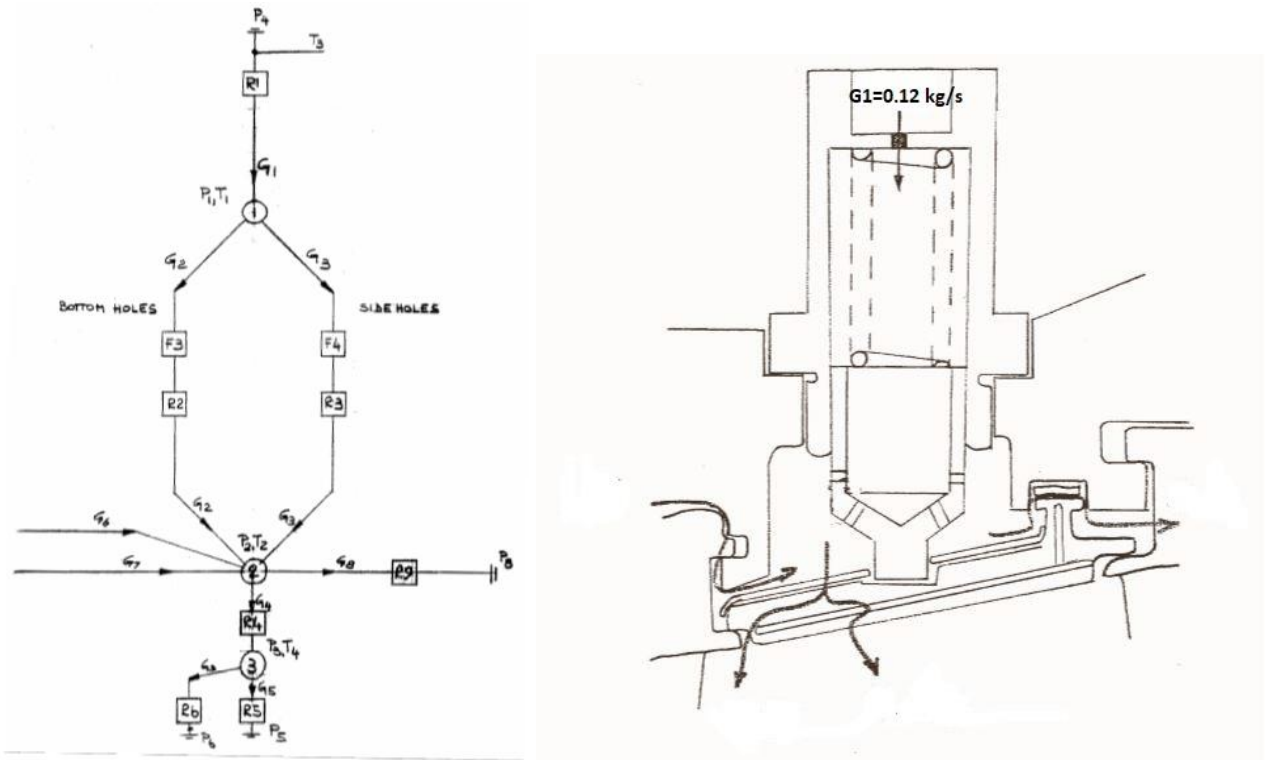

Figure 2.6.1.5 – Second ring segment cooling schematic representation.

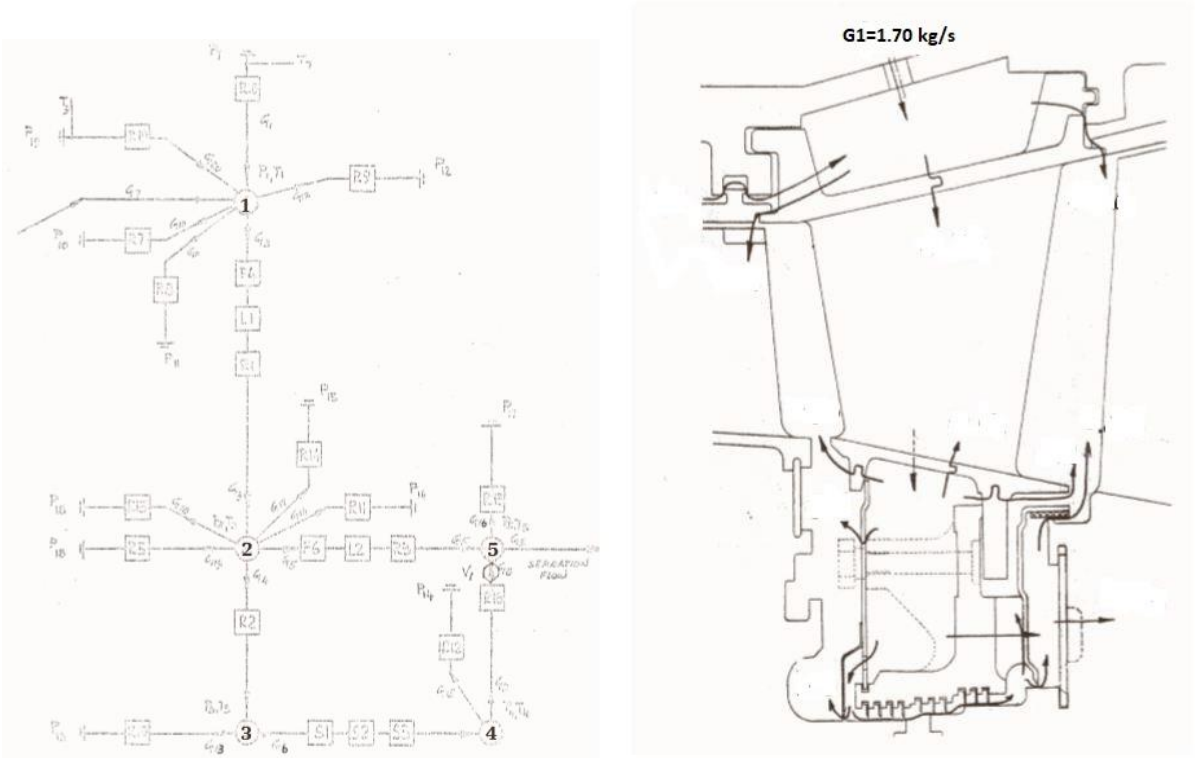

Figure 2.6.1.6 – Third vane cooling schematic representation.

2.6.2 Rotor cooling

In this Paragraph a description of the rotor cooling system is proposed. As previously mentioned, the cooling for the mod.3 configuration is a bit different from the standard configuration since the mod.2 is implemented as well. Therefore, a description and a schematic representation of the very last version is here-by presented.

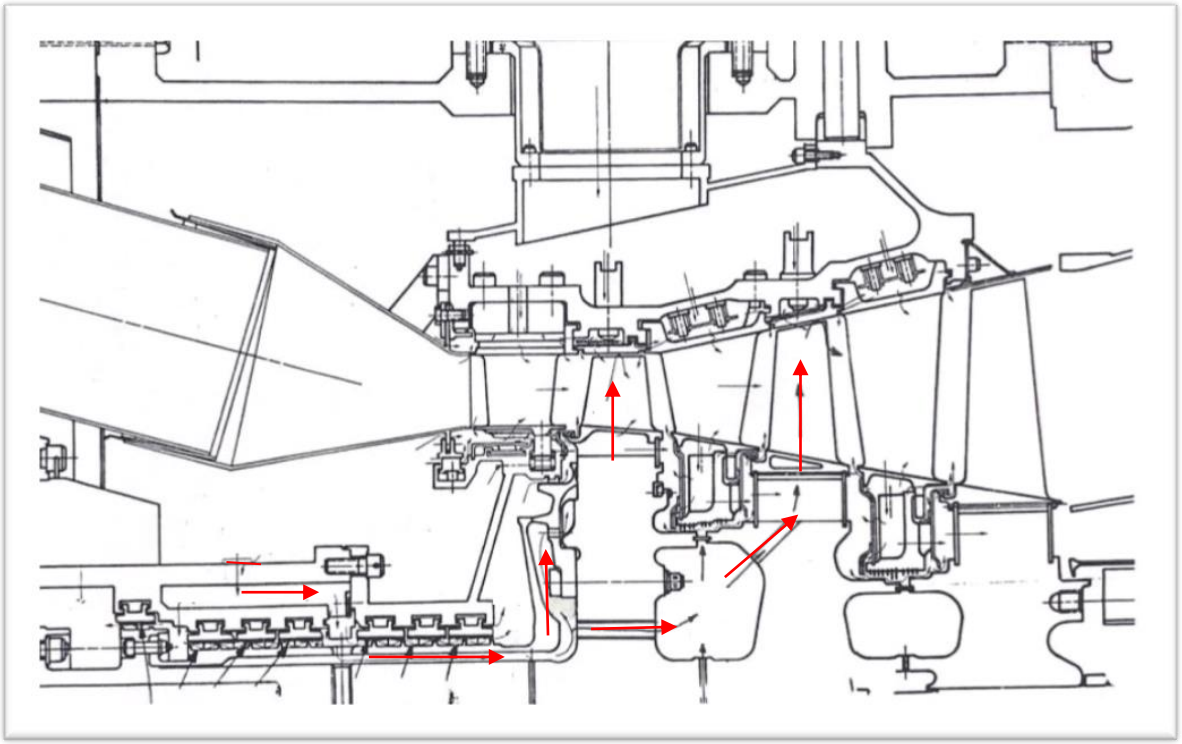

Figure 2.6.2 – Rotor cooling.

The air bled from the compressor delivery, which flows through an external cooler is consequently steered to the inlet of the rotor cooling circuit (red segment in the drawing above). The path followed is represented by the red arrows. As it is possible to notice, after the air flows through the air distribution ring (present between the two groups of sealings) continues following the path and is later divided. One part of it flows directly towards the upper part of the first disk where, through proper holes realised on it, feeds the first stage blades.
The other part instead is directed towards the second stage blades, still by means of holes realised on the first disk, but closer to the centre of the latter.
This configuration, relatively simple yet effective, allows to control the cooling of the rotating parts independently from the static ones, therefore a higher precision, efficiency and lower temperatures can be obtained.

3. Mean-line performance analysis

Given the aim of obtaining an increase of the performances by means of not invasive yet simple and effective modifications, a preliminary analysis of the machine has been carried out in order to evaluate which could have been the key parameters to act on and obtain the desired results.
This preliminary analysis has been translated into a sensitivity analysis carried out as a function of the turbine inlet temperature and the air mass flow rate bled from the compressor.
Furthermore, these initial analyses have been carried out from a mean-line standpoint in order to have a general idea of the behaviour of the machine and relied on the in-house developed software PH4145, historically used for this kind of analysis since the Seventies.
A brief description of the software is presented in the beginning, together with a brief mention on the matching characteristics of turbine and compressor, then the attention is focused on what the outputs of this software have been and the path followed for the successive modifications of the machine. [4]

3.1 Turbine and compressor characteristics matching

Given the structure of a turbo-gas plant, some theoretical considerations have to be made before proceeding with the analysis. In particular, the turbine and the compressor are axial machine characterised by a certain map, better saying that the single components are designed according to some procedures and their performances are obtained from actual tests.
Once these components are embedded in an engine, the range of all the feasible operating conditions is significantly reduced, therefore there is the problem to find the corresponding operating points on the characteristics of both the components when the engine is running at steady-state speed.

3.1.1 Compressor characteristic

Here-by axial compressor characteristic curves are reported. These compressors are well tailored for high mass flow rates, characterised by high efficiencies and limited space, that is why are the perfect choice for a turbo-gas plant.
The curves shown the compression ratio (ordinate axis) and isentropic efficiency as a function of the corrected mass flow rate (abscissa axis) and the corrected speed. In general, these last two terms are referred to a certain temperature and pressure values.

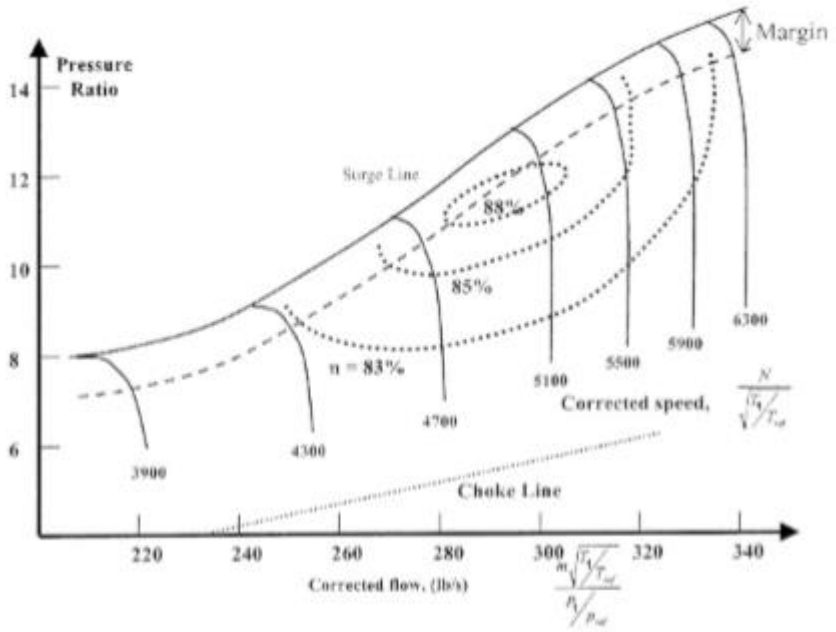

Figure 3.1.1.1 – Axial compressor characteristic.

On the map it is possible to appreciate the curves that report the compression ratio and the isentropic efficiency as a function of the corrected mass flow rate for given values of the corrected speed. There exists an upper limit to these curves, which is the so-called surge line. This curve intersects all the maxima of the corrected speed curve. This line represents a really critical condition since the compressor becomes unstable and the possibility of a reverse flow may take place.
One more interesting information is that the corrected speed curves appear almost independent from the corrected mass flow rate, which is a peculiarity of the axial compressors.
There is also present a lower limit for the characteristic curves which is mostly due to the choking conditions achievement in one or more compressor stages.
This phenomenon may lead to shocks and a significant reduction of the compressor efficiency.

3.1.2 Turbine characteristic

In order to deal with the turbine characteristic, an axial turbine is taken as reference. The characteristic curves of a turbine report the corrected mass flow rate value and isentropic efficiency as a function of the expansion ratio for given corrected rotational speeds.

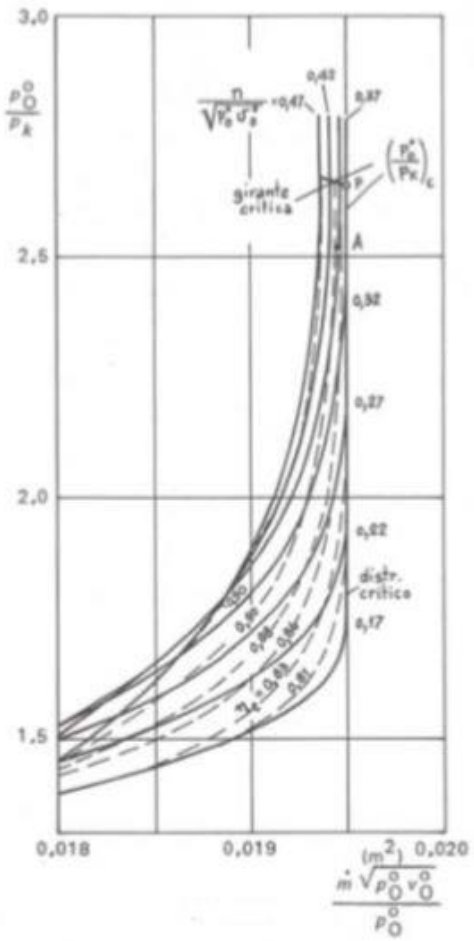

Figure 3.1.2.1 – Axial turbine characteristic.

The turbine inlet conditions shown in Figure 3.1.2.1 (T_O, p_O, v_O) are the total quantities and p_K represents the total outlet pressure. The graph shows the isentropic efficiency being not so sensitive to the expansion ratio variation and corrected speed. This is mostly due to the turbo-expander nature, for which the acceleration of the fluid produced by the expansion significantly reduces fluid vein detachment even for high incidence angle conditions. Furthermore, the efficiency is enhanced by the recovery effect, as heat dissipated due to friction can be partially transformed in work during the expansion.
The maximum value of the mass flow rate, Γ, is reached for expansion ratio such that the sonic condition (or choking) is reached in a turbine stage. Experimentally, it can be observed that in sub-critical conditions the curve can be modelled as a quarter of ellipse (Stodola law) where:

$$\Gamma = \Gamma_{cr} \quad if \quad \beta_t \le \beta_{cr} \tag{3.1.2.1}$$

$$\left(\frac{\Gamma}{\Gamma_{cr}}\right)^2 + \left(\frac{\beta_t - \beta_{cr}}{1-\beta_{cr}}\right)^2 = 1 \;\; if \;\; \beta_t > \beta_{cr} \tag{3.1.2.2}$$

where Γ_{cr} is the critical mass flow rate values obtainable for an expansion ratio equal to β_{cr}.

3.1.3 Matching condition

The working point of the turbo-gas can be found by representing the turbine characteristic on the compressor map, as the former is more easily representable being it independent from the rotational speed. Therefore, if the turbine characteristic is considered, it is possible to state that in the critical region Eq. 3.1.3.1 holds:

$$\beta = \frac{1}{\Gamma \eta_{\pi b}} \frac{(1+\alpha)}{\alpha} \sqrt{\frac{T_3}{T_1}} \frac{\dot{m}_a \sqrt{T_1}}{p_1} \tag{3.1.3.1}$$

This does mean that the turbine characteristic is a straight line passing through the origin of the map with a slope depending on the turbine inlet temperature, whereas in the sub-critical region the turbine characteristic is an ascending curve passing in the point (0,1) and tangent to the straight line above-mentioned in correspondence of the critical expansion ratio.
In Figure 3.1.3.1 the matching configuration is reported.

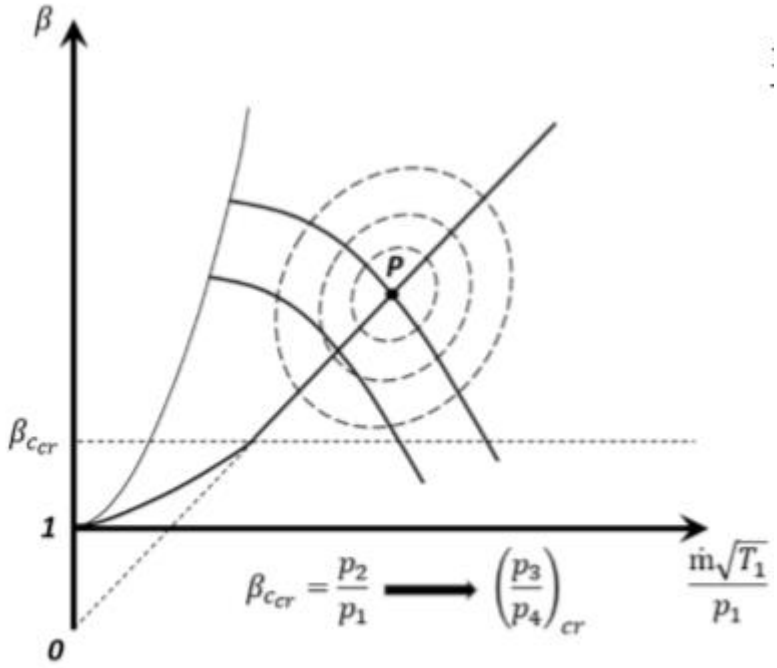

Figure 3.1.3.1 – Turbine and compressor characteristics matching.

From the intersection between the two curves it is possible to obtain the exact working point.

3.2 PH4145: software introduction

The software PH4145 is a FORTRAN code used in order to compute the expected performance of a single-shaft industrial gas turbine.
In the input part it is possible to set all the data of the machine, including the geometry, clearances, compressor map, cooling system arrangement, design working conditions, kind of fuel and so on.
Given the ambient temperature and the shaft actual rotational speed, the corrected rotational speed is obtained with respect to a reference temperature, therefore the position of this value is reported on the compressor map and, by quadratic interpolation, the corresponding curve is defined.
Once the compressor corrected speed, corrected mass flow rate, compressor ratio and compressor efficiency are fixed, the flow condition at the burner inlet are obtained.
For each point of the curve a guess value for the Stodola factor is supposed for the design condition, then the TIT (Turbine Inlet Temperature) is computed. As a function of it the fuel mass flow rate is computed and therefore the turbine inlet mass flow rate as well. Given these "first guess" values the turbine expansion computation starts.
Many loops are present, the TIT is kept fixed and the turbine mass flow rate is varied in order to get the desired expansion ratio. This turbine mass flow rate value is used in order to update the Stodola value, which is then used to compute a new TIT and starting a new loop.
The iteration ends when the difference between two successive Stodola values is lower than a certain tolerance.
In Figure 3.1.1 a schematic representation is given.

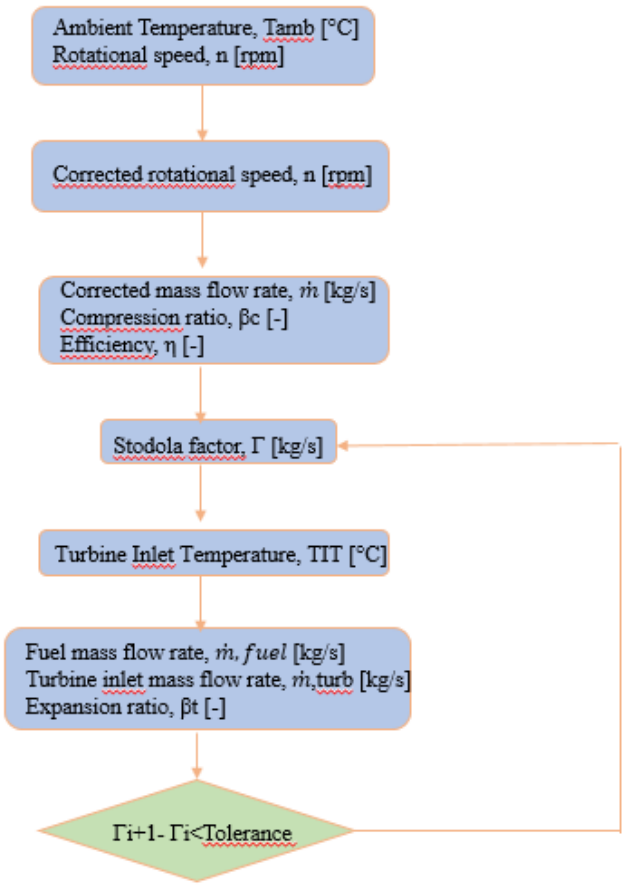

Figure 3.2.1 – PH4145 logic scheme.

A few words must be spent on the cooling logic as well. In particular, the software gives the possibility to insert as input values four types of cooling, which respectively are:

- Type 1, no-swirl flow, which involves all the secondary flows which are not in direct contact with a rotating part that enter in the main flow (blue in Figure 3.2.1);
- Type 2, swirl-flow, involving all the flows in direct contact with a rotating part that enter in the main flow (red in Figure 3.2.1);
- Type 3, involving the air mass flow rates flowing inside the stator and entering the main flow (orange in Figure 3.2.1);
- Type 4, involving the air mass flow rates flowing inside the rotor and entering the main flow (green in Figure 3.2.1).

Furthermore, the values are inserted as the mass fraction of the mass flow rate bled from the compressor.
All the four fractions have to be input for each row (six in the example, plus one corresponding to the flow entering at the end of the last row), whether it is a stator or a rotor and given the number of rows, the "cooling matrix" is obtained.
The values between the coloured rectangles correspond to the considered flow temperature (expressed in Rankine).
The term "cooling matrix" has been later used in order to deal with all the considerations made on the cooling system and consequent modifications to be done on the PH4145.

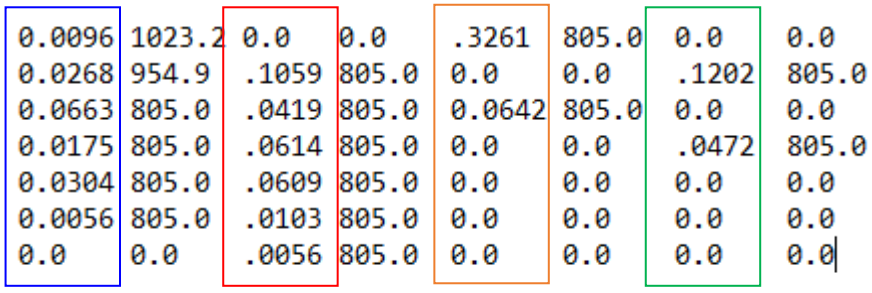

Figure 3.2.2 – Example of code, concerning the cooling set-up.

3.3 Mean-line sensitivity analysis

By relying on the PH4145 software, which allows to predict the behaviour of the machine from a thermodynamic, mean-line point of view, the analysis has been carried out as a function of some leading parameters.
For what concerns the present study, the parameters of interest considered have been the Turbine Inlet Temperature (TIT) and the air mass flow rate bled from the compressor necessary for the cooling system, considering ISO conditions (T_1=298 K, relative humidity RH=60 %).

The choice has fallen on these parameters as they are the most easily manageable from an operative point of view and can lead to the most profitable gain without the drawback of critical issues that can arise from more complex changes, at least on a first basis.
In particular, the change of the TIT is directly governed by the control system and once there is the certainty that a determined value cannot cause damage to the mechanical parts, no problems are present.
The change in the cooling air mass flow rate may be a little trickier, but once the cooling system is detailly analysed, it is easy enough to understand where it is possible to apply some modifications and where not.
In addition to this, the idea behind is to get an increase in the performances, which means to obtain an increased output power and a higher efficiency.

From a thermodynamic point of view, the targets can be obtained either by increasing the compression ratio, choice infeasible in this case as any modification on the compressor geometry can be delicate and becomes risky when there is not the possibility to experimentally test it, or by increasing the turbine inlet temperature, which is the path followed.

Furthermore, the cooling air mass flow rate in a certain sense represents a huge, but necessary waste, since the compressor has to perform work on it to increase its pressure level, but then this portion is not used to extract work in the turbine, moreover its “negative” effect is amplified by the fact that this mass flow rate mixes together with the principal flow, lowering its enthalpy level, therefore causing a decrease in the possibility to extract more work. Obviously, it is not possible to definitely eliminate the cooling air mass flow rate as the mechanical components must hold a certain temperature level at most in order to avoid creep phenomena and excessive deformations.
That is why the need of optimising the cooling system emerges.

In Figure 3.3.1-2 it is possible to appreciate the useful power and efficiency as a function of the mass flow rate bled from the compressor for different turbine inlet temperature levels.

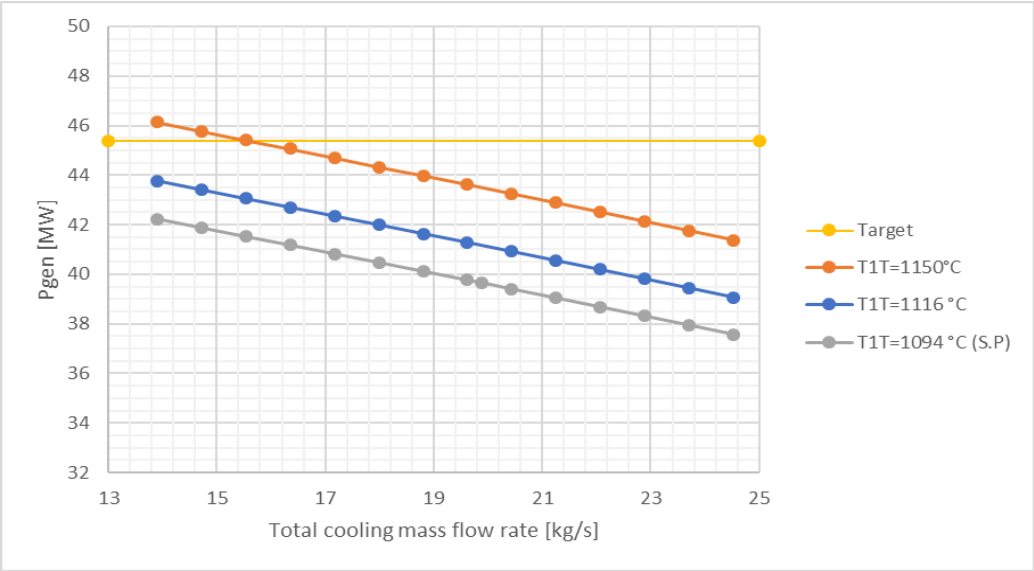

Figure 3.3.1 – Expected useful power trend.

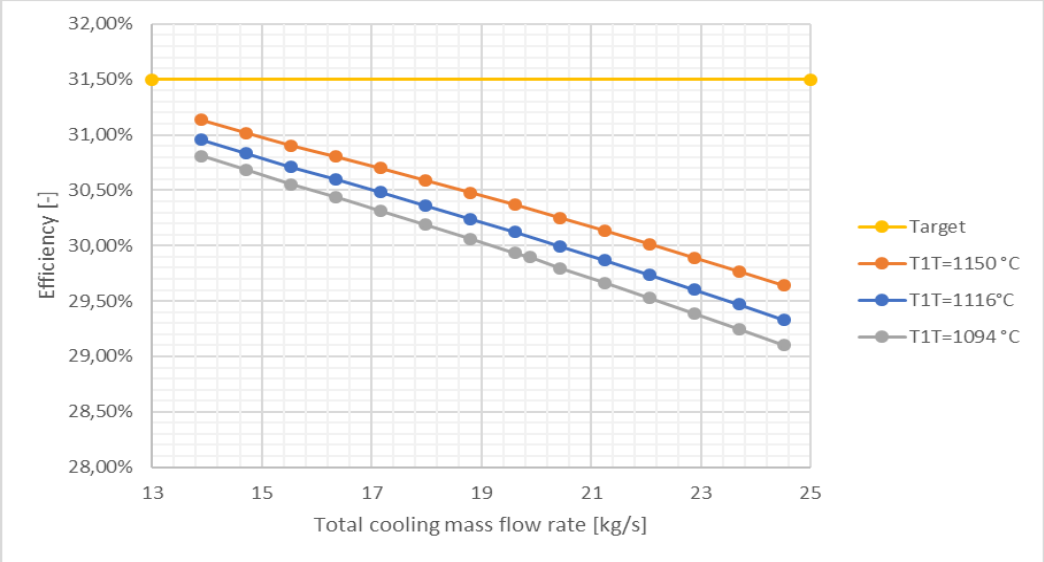

Figure 3.3.2 – Expected efficiency trend.

The total cooling mass flow rate boundaries have been deliberately assumed according to common sense; in fact, it is not possible to think to an exaggerated reduction in the cooling mass flow rate.
Limiting the analysis to this first study, it is possible to notice that the target power could be reached, even though it requires a reduction in the cooling mass flow rate from 19.9 kg/s to 15.5 kg/s.
Concerning the efficiency, the target seems unfeasible.
The next step consists in analysing the cooling system and verify whether or not it is possible to modify it in order to get a useful power increase.

3.4 Turbine Inlet Temperature increase

In order to have a proper idea of the magnitude of each effect, they have been considered separately. At first the turbine inlet temperature is considered, since the amount by which it has to be increased is known according to operative experience.

Table 3.4.1 – Machine parameters (UG, starting configuration).

Parameter	Value	Unit of measure
P_gen	39.7	[MW]
η_g	29.9	[%]
$T1T$	1367	[K]
T_{exh}	793	[K]
$T2C$	626.2	[K]
$P1T$	11.9	[bar]
$\dot{m}_a$	163.5	[kg/s]
$\dot{m}_{a,cool}$	19.9	[kg/s]
$\dot{m}_f$	3.2	[kg/s]
n	4918	[rpm]

Table 3.4.2 – Machine parameters (after TIT increase).

Parameter	Value	Unit of measure
P_gen	43.5	[MW]
η_g	30.3	[%]
$T1T$	1423	[K]
T_{exh}	824	[K]
$T2C$	633	[K]
$P1T$	12.0	[bar]
$\dot{m}_a$	163.5	[kg/s]
$\dot{m}_{a,cool}$	19.9	[kg/s]
$\dot{m}_f$	3.4	[kg/s]
n	4918	[rpm]

4. Cooling optimisation and performance improvement

The aim of this Chapter is to highlight which the cooling system modifications have been, the logic adopted, the consequent changes to be made from design and manufacturing point of view and the impact on the performances (always relying on the PH4145 software).
In order to be able to properly analyse the cooling system, the in-house software PH4165 has been necessary. It allows to model the single component or entire circuit flow network, giving reliable output (mostly pressures and flow rates).
A brief description of the code is presented [5] at first, then all the modifications will be presented one by one.

4.1 PH4165: software introduction

The software is able to solve complex flow networks inside Westinghouse project-based turbomachinery. It is used to estimate mass flow rates and pressures along cooling system inside the turbine. The network is modelled as a sequence of pipes (straight elements with just one entry and one exit) and chambers (elements in which two or more pipes converge). A flow is considered as a constant leakage to or from a chamber. For each pipe, seven different kinds of loss element may be handled:

- Pressure (P): pressure at the end of the pipe;
- Restriction (R): loss element with one velocity head loss;
- Fractional (F): loss element with a fraction of a velocity head loss;
- Seals (S): smooth labyrinth seals;
- Vortices (V): pressure change in radial direction due to solid body rotation;
- Friction (F): friction losses according to Moody diagram;
- Temperature (T): upstream temperature of the element.

Elements are then assembled in order, according to the real coolant path inside the machine.
The software requires an input geometry: loss elements characteristic, pressures and temperatures. Then it is asked to assume all internal chambers pressures and flow direction, and to specify tolerance for each chamber convergence. The PH4165 software follows an iterative procedure, using a “compressible adiabatic flow with losses” treatment, in order to calculate all intermediate pressures and actual flow direction. Each pipe is examined in two directions: in this way the software also handles cases for which flow direction is opposite with respect to the assumed one.
The main software limitation is that it is an iterative procedure based, so each result is affected by an uncertainty, depending on the tolerance set for each network chamber. Another limitation is that the software calculates air temperature variation along the channel, but heat balance in each chamber is not part of the main iteration, so it is neglected.

4.2 Rotor cooling set-up and modification

Before dealing with the actual modifications carried out on this delicate feature of the machine, it is necessary to state that a sort of set-up phase has been necessary.
In particular, as mentioned in Chapter 2, the machine has undergone different modifications. Concerning the rotor cooling and its PH4165 flow network, it has been necessary to put two aspects together, since they were considered separately:

- on the one hand the first blade cooling channel design had been changed [5] and, consequently the PH4165 source file;
- on the other one the cooling on the second blade (Paragraph 2.5) had to be considered as well.

The first part of the work dealt with in this Chapter has consisted in merging together these two aspects, modifying the PH4165 source file, aiming at obtaining a global configuration.
The final logic scheme can be appreciated in Figure 4.2.1.

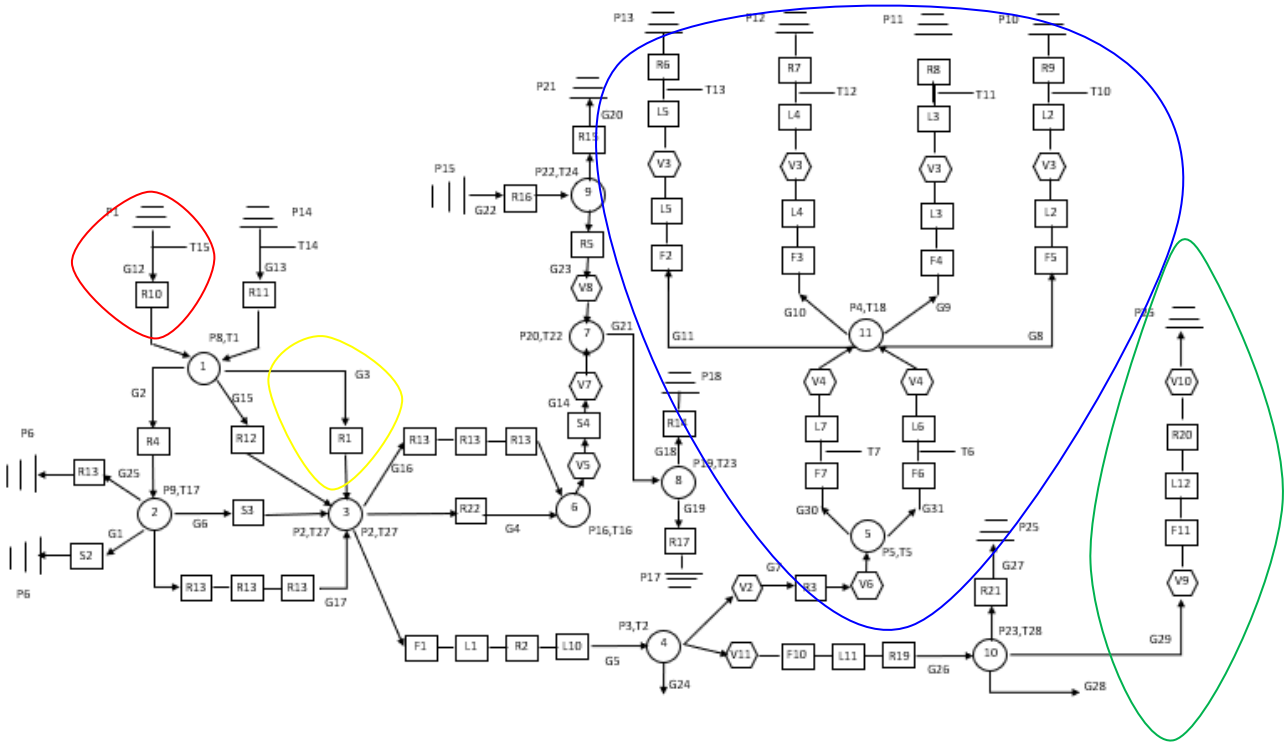

Figure 4.2.1 – Rotor cooling flow network.

The zone highlighted in blue represents the modelling of the first blade, without considering the leakages which are modelled on the closest left branches.
The green zone instead represents the cooling in the second blade.
In red, the total rotor cooling mass flow rate is considered, in yellow the net part (without leakages) that passes through the air distribution ring and feeds the circuit (Figure 2.6.2).

As the cooling in the second blade is introduced, a higher cooling mass flow rate is necessary and, consequently a performance lowering is expected. In Table 4.2.1 the characteristic parameters are reported.

Table 4.2.1 – Machine parameters (after cooling introduction on the second row blade).

Parameter	Value	Unit of measure
P_gen	42.8	[MW]
η_g	30.0	[%]
T1T	1423	[K]
T_{exh}	823	[K]
T2C	631	[K]
P1T	11.9	[bar]
$\dot{m}_a$	163.5	[kg/s]
$\dot{m}_{a,cool}$	21.2	[kg/s]
$\dot{m}_f$	3.4	[kg/s]
n	4918	[rpm]

On the bright side, as the second row blade is cooled directly from the rotor cooling, there is no more the need to cool it from the second vane, therefore the need of changing the PH4165 source file and think about design modifications accordingly emerged.
According to Figure 2.6.1.4, representing the logical scheme of the second vane, the mass flow rate G 8 has been reduced down to zero.
This modification obviously has led to the need to rebalance all the flow rates and pressures, as the idea behind is to keep unchanged all the flow rates, except for the ones that is necessary to eliminate or reduce.
For this reason, in order to rebalance all the flow rates, some changes should be made from a manufacturing point of view:

- no through holes have to be present on the seal ring (R 3);
- the clearance between the second disk and the seal ring (R 4) has to be reduced;
- a higher honeycomb thickness (R 6) is necessary;
- the clearance between the labyrinth seal and the second disk (S 3) has to be reduced.

The exact values will not be reported here, as they are privileged information.
In the end these modifications lead to a G 9 reduction of 10.9 %.

Still considering the rotor cooling circuit, after a deep analysis of all the flow rates computed in the latter, the output results have made the situation clear enough to determine which leakages could be reduced.
In particular, the mass flow rate G 20 (Figure 4.2.1) resulted to be too high and not useful since it corresponds to a flow leaked between the blades due to a clearance presence of an elevated magnitude. The cooling flow did not encounter a high resistance, or equivalently a small restriction, in correspondence of the lateral part of the blade root, therefore a waste was present as it was not full employed from a cooling point of view.
The solution to this problem has consisted in a redesign of the blades (to be still carried out in practice) of the first stage by introducing a sealing pin between the blades, which, during hot working, gets centrifugated closing as much as possible the passage. The criterion through which the new restriction has been computed and its value will not be presented here as it is a privileged information, the key point is that the restriction R 15 of the sketch has been reduced.
Due to this higher flow resistance a backpressure took place, generating a pressure increase in chambers 6 and 7, therefore the idea to rebalance the pressure values consisted in substituting the labyrinth seal S 1 with a restriction (R 22) that simulates a brush seal. This foresight would allow a pressure rebalancing.
Consequently, as the aim is to reduce the G 1 and G 12 mass flow rates, the air distribution ring holes diameter has been reduced by 17 % thus leading to a net mass flow rate reduction of 21.0 %.
In the end, an overall mass flow rate reduction has been still obtainable, generating a power increase. The machine interest parameters are reported in Table 4.2.2.

Table 4.2.2 – Machine parameters (after cooling system modifications).

Parameter	Value	Unit of measure
P_gen	44.0	[MW]
η_g	30.5	[%]
$T1T$	1423	[K]
T_{exh}	828	[K]
$T2C$	634	[K]
$P1T$	12.1	[bar]
$\dot{m}_a$	163.5	[kg/s]
$\dot{m}_{a,cool}$	18.7	[kg/s]
$\dot{m}_f$	3.4	[kg/s]
n	4918	[rpm]

As last step concerning the rotor cooling modifications, the turbulation of the blades of the first stage has been modelled as necessary passage of another complementary thesis [7], and afterwards implemented on the PH4165 source file.
Just as a brief introduction, the turbulation is a machining operation, generally applied to the turbine blades, consisting in realising cooling channels characterised by alternatively larger and smaller cross-section areas, so as to increase turbulence and consequently the heat transfer coefficient, thus allowing a reduction in the needed cooling mass flow rate. A turbulated channel section view can be appreciated in Figure 4.2.2. The diameter *D*, pitch *p* and rib thickness *e* are indicated.

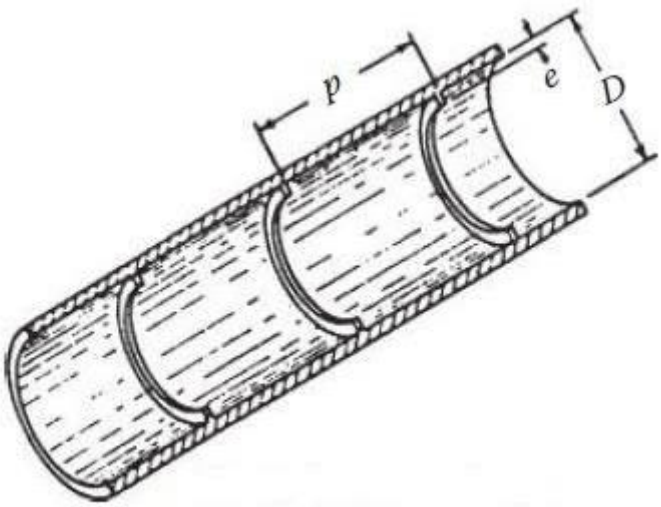

Figure 4.2.2 – Turbulated channel.

The modification implemented on the PH4165 has brought to a reduction in the mass flow rate (G 7 in Figure 4.2.1) of about 24 %. The machine interest parameters are reported in Table 4.2.3.

Table 4.2.3 – Machine parameters (first stage blades turbulation).

Parameter	Value	Unit of measure
P_gen	44.2	[MW]
η_g	30.5	[%]
T1T	1423	[K]
T_{exh}	829	[K]
T2C	635	[K]
P1T	12.1	[bar]
$\dot{m}_a$	163.5	[kg/s]
$\dot{m}_{a,cool}$	18.0	[kg/s]
$\dot{m}_f$	3.4	[kg/s]
n	4918	[rpm]

Just to have a more straightforward idea of the results achieved, at least from a theoretical point of view, a direct comparison between the starting point machine configuration and the one after all the modifications is reported in Table 4.2.4.

Table 4.2.4 – Machine parameters comparison.

Parameter	**Starting configuration**	**After cooling system modification and turbulation**	**Unit of measure**
P_gen	39.7	44.2	[MW]
η_g	29.9	30.5	[%]
$T1T$	1363	1423	[K]
T_{exh}	793	829	[K]
$T2C$	626	635	[K]
$P1T$	11.9	12.1	[bar]
$\dot{m}_a$	163.5	163.5	[kg/s]
$\dot{m}_{a,cool}$	19.9	18.0	[kg/s]
$\dot{m}_f$	3.2	3.4	[kg/s]
n	4918	4918	[rpm]

5. Stream-line performance analysis

The last step of this thesis consists in a streamline analysis of the turbomachine. This is necessary in order to have a more detailed idea of the flow evolution inside the turbine, given the bidimensional approach (the axial dimension and the radial one as well are considered) and analyse possible critical conditions concerning the flow path. This puts the basis for a complete thermo-structural verification to be carried out by means of a FEM approach which then could validate or not all the modifications previously assumed.
In order to carry out the stream-line analysis, the software AxSTREAM® has been used. A brief description is presented to make the reader understand the program logic and which the key passages have been.
In fact, before being able to perform the streamline analysis, a sort of alignment towards the PH4145 has been necessary. As AxSTREAM® gives the possibility to perform a mean-line analysis as well, the idea behind has been the one of having reasonably similar outputs from both the softwares in the mean-line condition and then to study the machine from a bidimensional point of view.
Furthermore, the model of the turbomachine was previously created on AxSTREAM® but the mean-line outputs, compared to the PH4145 ones were pretty different. This divergence mostly consisted in a wrong cooling set-up and wrong choice of blade clearances, as will be clearer later.

5.1 AxSTREAM®: software introduction

AxSTREAM® is a platform created by "SoftinWay Inc." meant for conceptual design, analysis and optimisation of radial, axial and mixed turbomachines. This software allows to have a simplified and embedded approach for turbomachinery design as the user is able to combine different phases, independent from each other, in order to create a single elaboration chain [6].
Concerning the turbomachine preliminary design, the software allows to develop the complete flow-path geometry, including the air-foil geometry, starting from the initial thermodynamic parameters (inlet and outlet), geometric constraints, mass flow rate and rotational speed.
As regards optimisation module instead, it is possible to determine a theoretical working model of the real machine starting from the 3-D CAD geometry by means of the AxSLICE module and the boundary conditions which can always be modified as a function of geometric or thermo-fluid-dynamic parameters.
By means of suited modules, it is also possible to carry out structural analyses, modal analyses and to create a Campbell diagram able to show the rotational speeds dangerous for the system.
One aspect more to be highlighted is that the software allows the model constructions by groups, this means that compressor and turbine have to be analysed separately. Moreover there is the possibility to use the solver preserving the geometry, having at disposal two paths: on the one hand the iteration starts computing the mass flow rate for a given inlet pressure (turbine) or outlet pressure (compressor), on the other one the mass flow rate can be selected as non-varying parameter and the pressure values are consequently computed.

For what concerns the cooling, it is modelled through the "G-sigma data set" starting from the bleeding conditions ("0" suffix) through an isenthalpic throttling and corresponding pressure drop and successive heat exchange at a constant pressure, as shown in Figure 5.1.1.

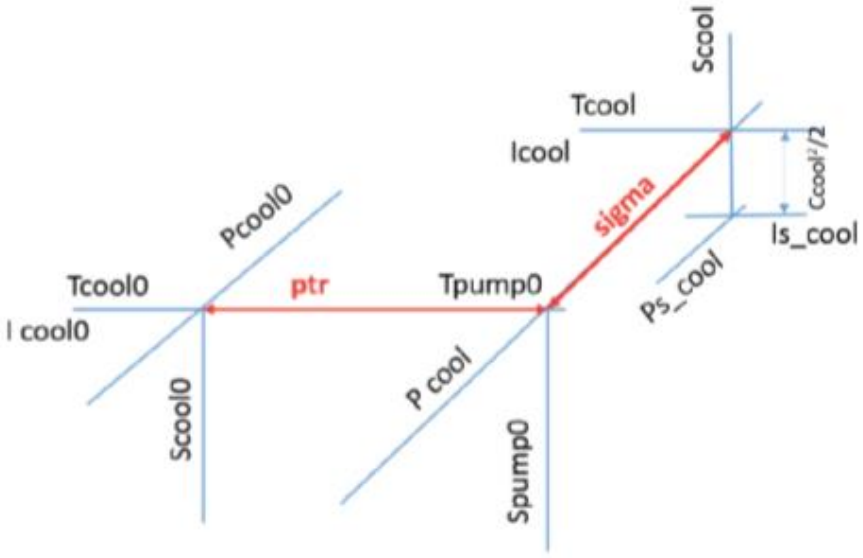

Figure 5.1.1 – Cooling air mass flow rate thermodynamic transformation.

For the model used by the software it is necessary to define some input values.
Thermodynamic input values:

- Air cooling mass flow rate;
- Total bleeding pressure;
- Total bleeding temperature.

Geometric input values:

- Cross section area of all the channels;
- Cooling channels angle with respect to a reference system;
- Radial position of the centre of mass of the cooling channels;
- Loss coefficients.

Non-dimensional input parameters:

- Sigma which represents the efficiency of the heat exchange at a constant pressure. It is defined as the ratio between the temperature increase of the cooling flow in the channel and the temperature difference of the principal flux at the row inlet and the cooling flow temperature at the beginning of the channel. (Eq. 5.1.1)

$$sigma = \frac{T_{cool} - T_{pump0}}{T_{in\_main} - T_{pump0}} \tag{5.1.1}$$

  This parameter shows a great importance in the cooing model validation and in general it is assumed according to operative experience.

In the cooling set-up, it is necessary to respect the logic the software shows, trying to be as faithful to reality as possible, in fact the software, for the stators, offers the possibility to set as input parameters four kind of flows Figure 5.1.2:

- Internal endwall cooling;
- External endwall cooling;
- Leading edge cooling;
- Trailing edge cooling.

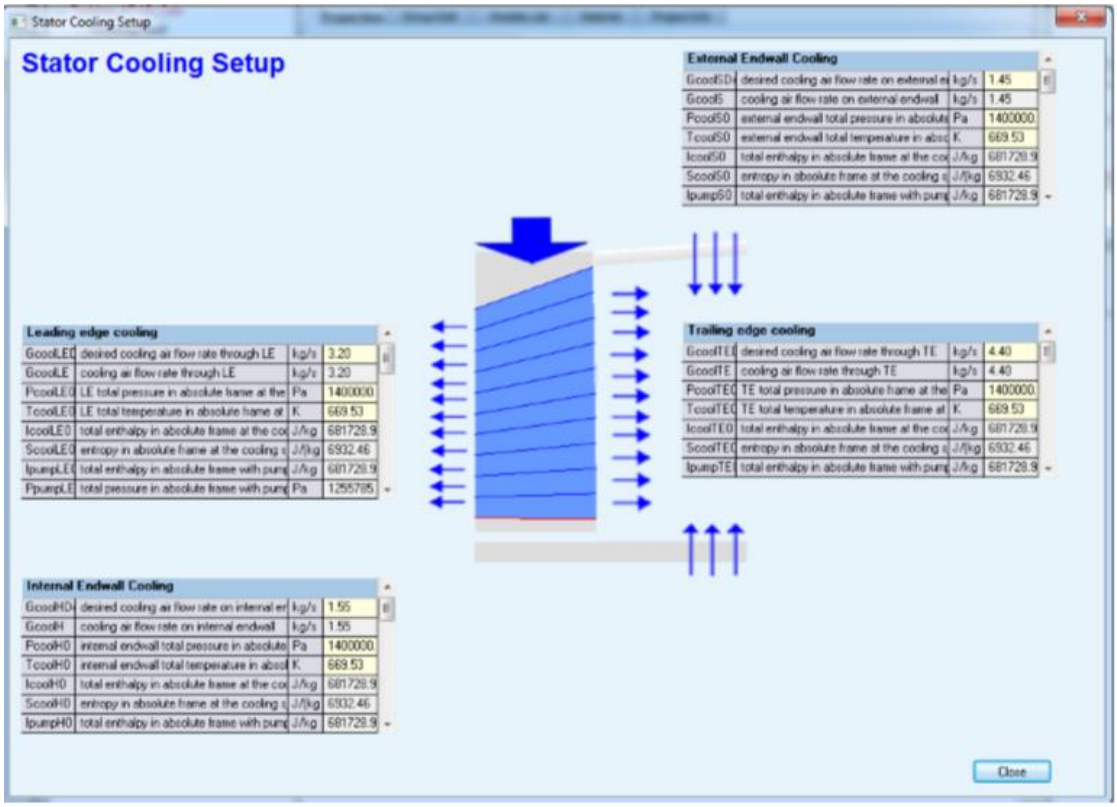

Figure 5.1.2 – Stator cooling set-up example.

Similar considerations hold for the rotor cooling as well, where in addition to the previous four flows, there is also the tip cooling flow (Figure 5.1.3)

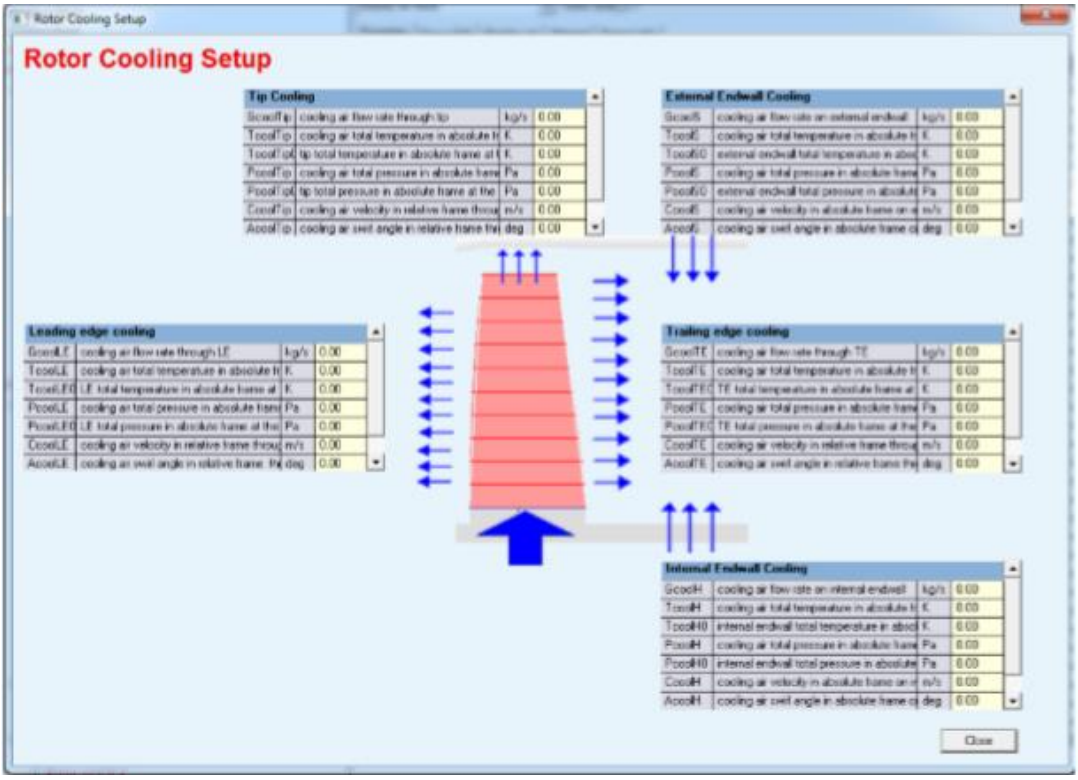

Figure 5.1.3 – Rotor cooling set-up example.

5.2 AxSTREAM® and PH4145 mean-line alignment

To carry out the first comparison the standard configuration of the machine has been taken in account (TG20 B7/8 UG).

As previously mentioned, some incongruencies were present in the AxSTREAM model of the machine, particularly regarding the clearance values and the cooling set-up criterion.
To face these problems some considerations have been made:

- For the clearances the solution has been quite simple, in the sense that on AxSTREAM, as in the PH4145, there is the possibility to directly insert the value representing the distance between the blade tip and the ring segment, therefore these two values have been posed equal according to the value already present on the PH4145;
- For the cooling set-up criterion, the solution has been a bit more complex. The idea behind has been to build the same conditions for the two software. For this reason, all the PH4165 flow networks have been deeply analysed, in order to understand which the cooling mass flow rates mixing with the principal flux were and then the corresponding values have been rearranged (summed or splitted) to adapt them to AxSTREAM control volume logic previously described.

These foresights have allowed the construction of a more realistic model.
Once the cooling parameters and clearances of the starting configuration of the machine have been assessed on AxSTREAM as well, a sensitivity analysis has been carried out as a function of the Turbine Inlet Temperature. As the compressor group is treated separately from the turbine one, the following procedure has been followed in order to guarantee the matching between the two of them.

- The turbine performances have been evaluated by imposing the mass flow rate, thus obtaining the pressure among other thermodynamic parameters as output;
- Known the turbine inlet pressure, this value has been divided by the pneumatic efficiency of the burner, thus obtaining the desired outlet pressure of the compressor;
- The compressor performances have been evaluated by imposing the outlet pressure and finding the mass flow rate;
- The consistency of the mass flow rates entering the compressor and exiting the turbine has been verified.

In Table 5.2.1-3 the comparisons for three different temperatures is reported.

Table 5.2.1 – PH4145 and AxSTREAM output comparison (TIT=1323 K).

Parameter	**PH4145**	**AxSTREAM**	**Unit of measure**	**ε_{rel} [%]**
P_gen	36.6	35.7	[MW]	2.46 %
T1T	1323	1323	[K]	-
T_{exh}	764	800	[K]	-4.70 %
T2C	624	632	[K]	-1.23 %
P1T	11.5	11.4	[bar]	0.87 %
$\dot{m}_a$	163.5	163.5	[kg/s]	-
$\dot{m}_f$	3.0	3.0	[kg/s]	-
n	4918	4918	[rpm]	-

Table 5.2.2 – PH4145 and AxSTREAM output comparison (TIT=1367 K).

Parameter	**PH4145**	**AxSTREAM**	**Unit of measure**	**ε_{rel} [%]**
P_gen	39.7	38.7	[MW]	2.52 %
T1T	1367	1367	[K]	-
T_{exh}	790	830	[K]	-5.06 %
T2C	628	635	[K]	-1.11 %
P1T	11.7	11.6	[bar]	0.85 %
$\dot{m}_a$	163.5	163.5	[kg/s]	-
$\dot{m}_f$	3.2	3.2	[kg/s]	-
n	4918	4918	[rpm]	-

Table 5.2.3 – PH4145 and AxSTREAM output comparison (TIT=1423 K).

Parameter	**PH4145**	**AxSTREAM**	**Unit of measure**	**ε_{rel} [%]**
P_gen	43.5	42.4	[MW]	2.53 %
T1T	1423	1423	[K]	-
T_{exh}	824	867	[K]	-5.22 %
T2C	633	639	[K]	-0.95 %
P1T	12.0	11.9	[bar]	0.83 %
$\dot{m}_a$	163.5	163.5	[kg/s]	-
$\dot{m}_f$	3.4	3.4	[kg/s]	-
n	4918	4918	[rpm]	-

The results divergence, indicated by ε_{rel} has been computed according to the following:

$$\varepsilon_{rel} = \frac{q_{PH4145} - q_{AxSTREAM}}{q_{PH4145}} \tag{5.2.1}$$

where q indicates a general quantity. No percentage is written if the parameter has been imposed as input.

As it is possible to notice from Tables 5.2.1-3, results are close even though not exactly equal.
This difference can be explained by the fact that the two software are completely different in the way input parameters and machine geometry are set, in addition to this there is an age difference of about 40 years.

On the one hand the PH4145 requires the geometric informations to be put in a specific place in the source file, generally they are acquired from drawings and referred only to a specific section of the air foil, AxSTREAM instead allows the importation of the geometry by means of a slicing technique able to recreate the air foil geometry along the radial direction section by section (it is possible to use seven sections at most), even though it may happen to adjust some specific points manually.

Furthermore, the compressor and turbine on AxSTREAM are treated as separated groups, while instead they are treated as a whole on the PH4145.

The PH4145 is obviously less detailed than AxSTREAM, which is a new generation software, in continuous updating, it is possible to use different models for cooling and losses calculation and, given the closed structure of the former, it is improbable to recreate the exact same conditions.

Nonetheless the results are reliable being the divergence reasonable and almost constant as the temperature varies. On the top of that, it is shown in Table 5.2.4-6, the error keeps constant as the cooling machine configuration changes, giving credit to the approach used and the results reliability.

In Table 5.2.4-6 the comparisons for three different cooling configurations is reported.

Table 5.2.4 – PH4145 and AxSTREAM output comparison
(Starting configuration, $\dot{m}_{cool}$ =19.9 kg/s).

Parameter	**PH4145**	**AxSTREAM**	**Unit of measure**	**ε_{rel} [%]**
P_gen	39.7	38.7	[MW]	2.52 %
T1T	1367	1367	[K]	-
T_{exh}	790	830	[K]	-5.06 %
T2C	628	635	[K]	-1.11 %
P1T	11.7	11.6	[bar]	0.85 %
$\dot{m}_a$	163.5	163.5	[kg/s]	-
$\dot{m}_f$	3.4	3.4	[kg/s]	-
n	4918	4918	[rpm]	-

Table 5.2.5 – PH4145 and AxSTREAM output comparison
(Cooling leakages reduced, $\dot{m}_{cool}$ =18.7 kg/s).

Parameter	**PH4145**	**AxSTREAM**	**Unit of measure**	**ε_{rel} [%]**
P_gen	44.0	43.5	[MW]	1.14 %
T1T	1423	1423	[K]	-
T_{exh}	828	870	[K]	-5.05 %
T2C	634	640	[K]	-0.5 %
P1T	12.1	12.0	[bar]	0.85 %
$\dot{m}_a$	163.5	163.5	[kg/s]	-
$\dot{m}_f$	3.4	3.4	[kg/s]	-
n	4918	4918	[rpm]	-

Table 5.2.6 – PH4145 and AxSTREAM output comparison
(Turbulation addition, $\dot{m}_{cool}$ =18.0 kg/s).

Parameter	**PH4145**	**AxSTREAM**	**Unit of measure**	**ε_{rel} [%]**
P_gen	44.2	43.8	[MW]	0.90 %
T1T	1423	1423	[K]	-
T_{exh}	829	872	[K]	-4.93 %
T2C	635	640	[K]	-0.79 %
P1T	12.1	12.0	[bar]	0.85 %
$\dot{m}_a$	163.5	163.5	[kg/s]	-
$\dot{m}_f$	3.4	3.4	[kg/s]	-
n	4918	4918	[rpm]	-

5.3 Stream-line analysis

The stream-line analysis represents the final point of this thesis, as it allows a deep understanding of the evolution of the flow path inside the machine.
This is mostly due to the fact that the approach followed is a bidimensional one, giving the possibility to understand how the thermodynamic parameters change along the axial direction and along the radial one as well. In fact, given the dimensions of the machine vanes and blades not negligible with respect to the wheels, it may be reductive or even not correct to apply the 1-D theory.
Furthermore, the necessity arises from the willing and need of having a relatively precise temperature trend along each component of the turbine in order to properly set the boundary conditions necessary for the thermo-structural validation.
In addition to this, some critical aspects that could be confined to determined zones can be now visible, thus allowing to be fully aware of them, to evaluate their effects and possibly to take decisions against them.
In Figures 5.3.1-2 the turbine temperatures trend for initial and final conditions are reported.

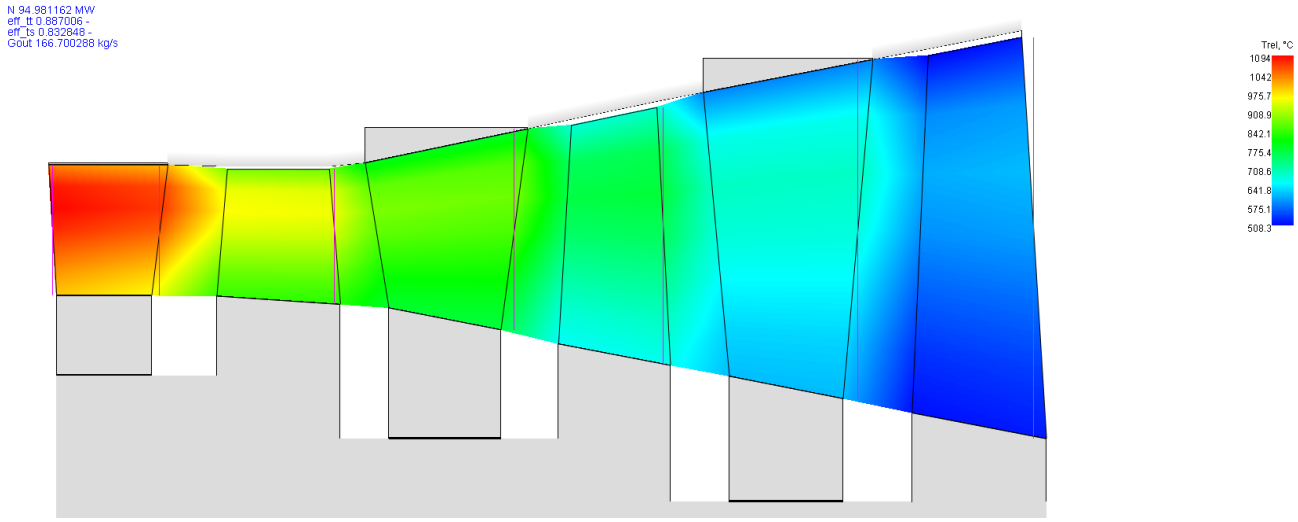

Figure 5.3.1 – Temperature trend, starting configuration (TIT=1094°C, $\dot{m}_{cool}$ =19.9 kg/s).

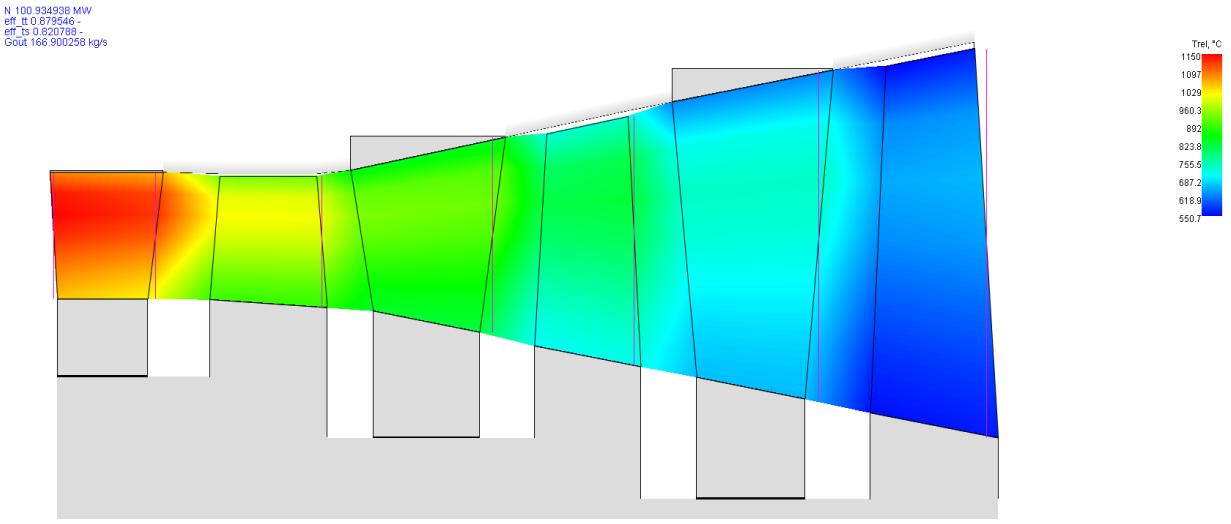

Figure 5.3.2 – Temperature trend, final configuration

(TIT=1150°C, $\dot{m}_{cool}$ =18.0 kg/s).

As it is possible to notice there is a considerable exhaust temperature increase between the two configurations.

This can be explained by the fact that the blade and vane aerodynamic profiles have not been redesigned in order to deal with the temperature increase, thus not being able to fully exploit the TIT increase. In fact, since the vane approximately behaves as an isentropic nozzle, as the temperature increases, the fluid velocity at its outlet (coincident to the one of the rotor inlet) increases as well, according to the first law of thermodynamics.

$$c_{vane\_outlet} = c_{rotor\_inlet} = \sqrt{2c_p (T^o_{IT} - T_{vane\_outlet})} \qquad (5.3.1)$$

Being the geometry unchanged, the aerodynamic blade profile is not the optimal one to deal with this speed increase. In Figures 5.3.3-4 the velocity triangles can be appreciated.

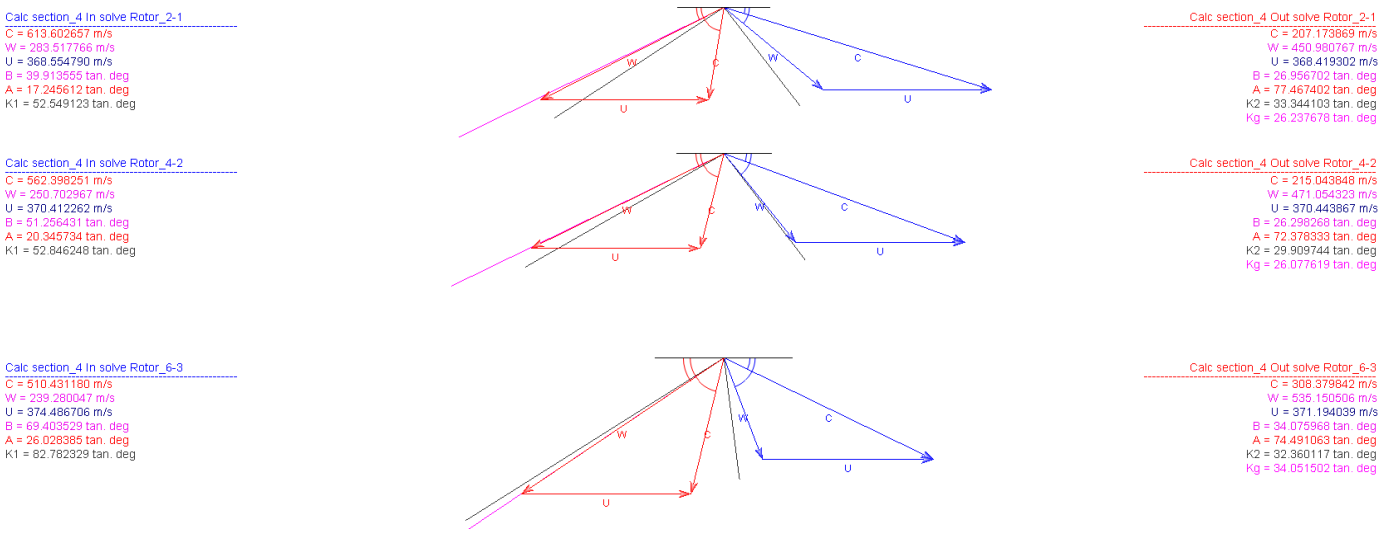

Figure 5.3.3 – Velocity triangles, starting configuration (Section 4 is considered).

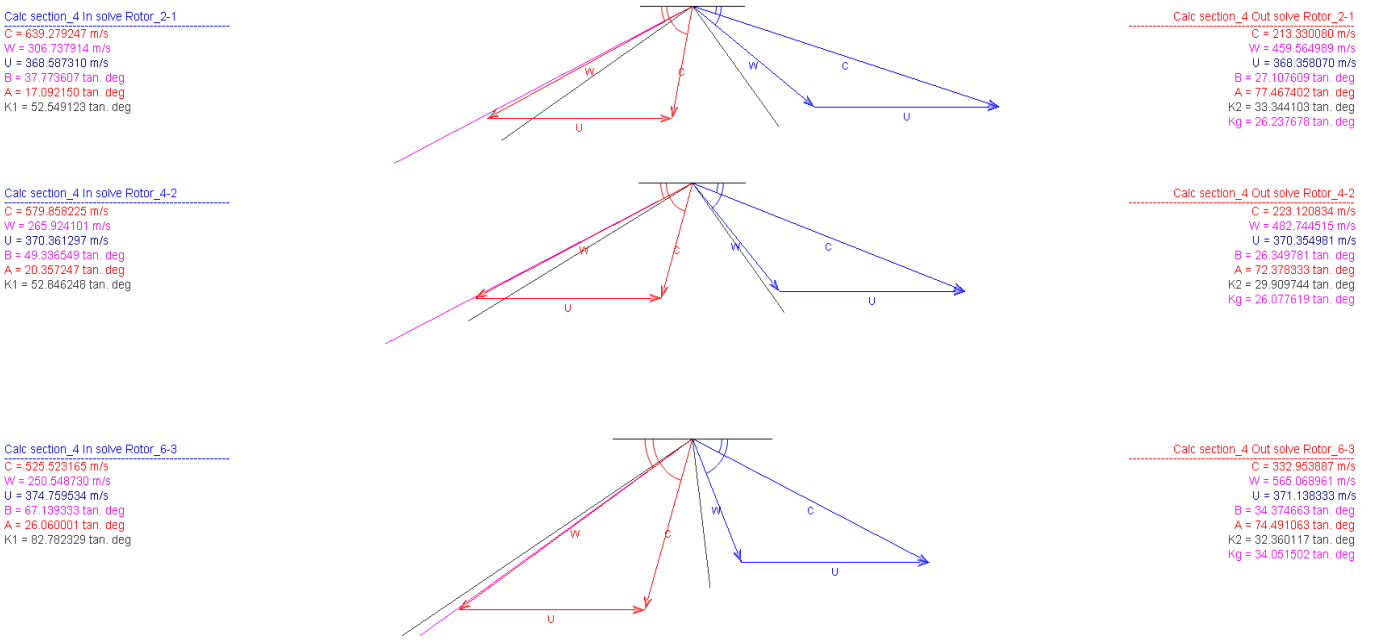

Figure 5.3.4 – Velocity triangles, final configuration (Section 4 is considered).

As it can be noticed, there is a decrease of the relative velocity angle β_1 corresponding to the inlet rotor section.

The exhaust temperature increase, apart from leading to a decrease in the turbine total-to-total and total-to-static efficiencies (eff_tt and eff_ts in the pictures), may lead to collateral manufacturing and working problems as well, as the mechanical components present in the exhaust part, which in the past had shown some criticalities due to temperature deformations, may fail.

The Mach numbers comparison has been considered as well. As it is possible to notice in Figures 5.3.5-6 the situation is pretty similar in both the starting and final configuration, a slight increase takes place in the final configuration.

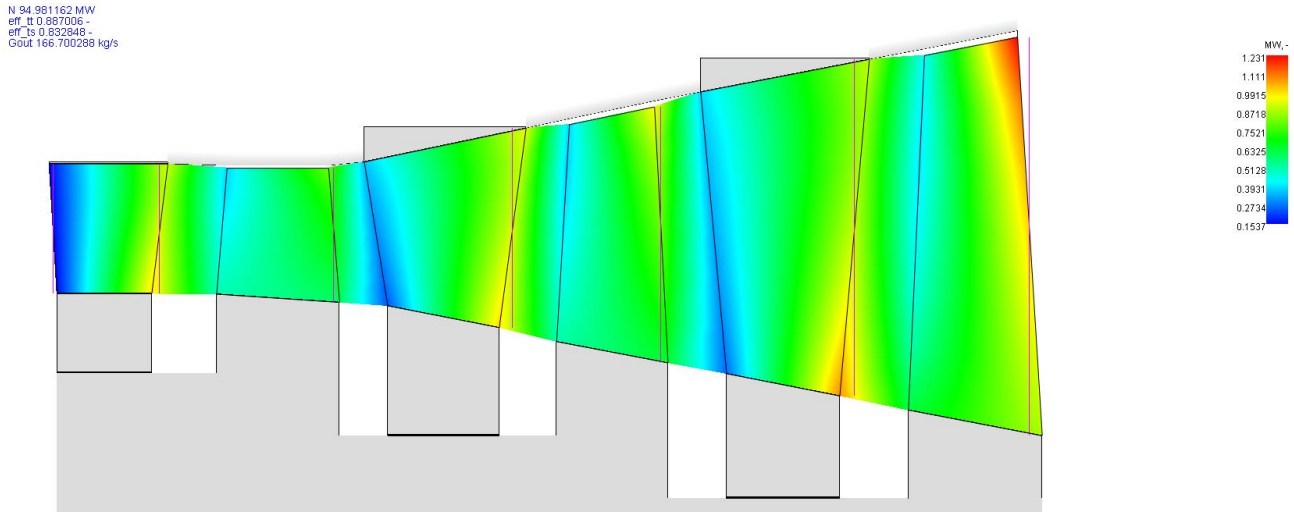

Figure 5.3.5 – Mach numbers, starting configuration.

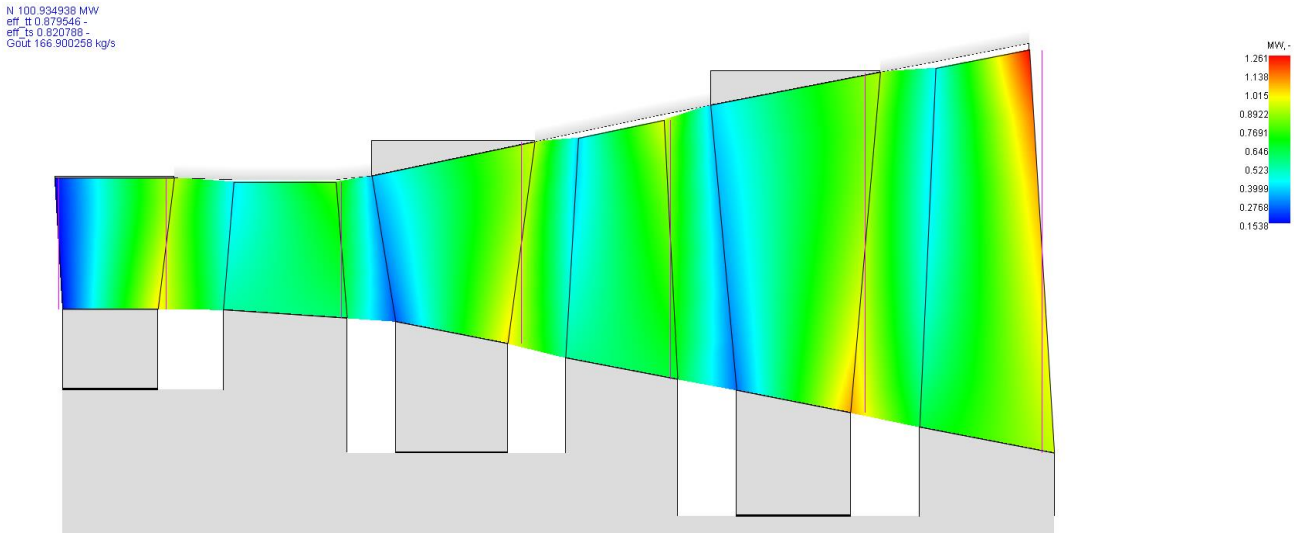

Figure 5.3.6 – Mach numbers, final configuration.

One critical aspect is that Mach numbers appear to be high at the base of the third vane and at the top of the third blade, thus leading to turbine efficiency decrease due to the possible generations of shocks.

Conclusions

Summing up:

- the initial sensitivity analysis has allowed to understand which direction had to be followed in order to obtain a performance increase, evidencing the possible limitations, therefore the turbine inlet temperature has been increased and cooling air mass flow rate reduced;
- in order to reduce the mass flow rate, a deep analysis of the cooling system (stator cooling and rotor cooling) has been carried out. The necessity to implement the cooling on the second blade through the rotor cooling system has brought some drawbacks counterbalanced by the possibility of reducing the cooling air mass flow rate on the second vane, managed by the stator cooling. The design choices (Paragraph 4.2) that should be made in order to deal with these modifications are relatively simple from the manufacturing point of view, thus avoiding a complete re-design of the production chain and low-cost as well, thus leading to a higher competitivity on the market.
  A first blade partial re-design should be done as well in order to allow the leakages reduction in the inter-blade zone, being the air waste not negligible at all, so as to obtain, in the end, a considerable power increase.
  Still concerning the first blade, the turbulation of the internal cooling channels of the blades may lead to interesting results, in fact an additional reduction of the cooling air mass flow rate may be obtained, still guaranteeing the blade heat dissipation capacity due to the increased heat exchange coefficient and consequently its thermo-structural resistance;
- a software alignment has been obtained (PH4145 and AxSTREAM) by focusing the attention on the machine parameters (geometric, thermodynamic) and particularly the cooling matrices. The advantage is on the one hand to validate all the considerations made by using the mean-line approach (PH4145) and on the other one to obtain a machine model suited for a successive stream-line analysis, able to evidence possible criticalities and supply the necessary outputs, mostly temperature trends, for the thermo-structural verification;
- in the end the stream-line analysis has been carried out, and the initial and final configurations of the machine have been compared. A decrease of both total-to-total and total-to-static efficiency has taken place, connected to the fact that the increase of the turbine inlet temperature has naturally led to an increase of the absolute speed at the first rotor inlet. Being the air foil profile unchanged with respect to the initial configuration, it can be stated that the former is not well-tailored to the new kinematic conditions and unable to fully exploit the fluid energy. Due to this aspect, an exhaust gas temperature increase has taken place as well, thus creating the need of carefully consider the stresses and strains the exhaust part, already critical, is subjected to.
  From the Mach numbers analysis, both in the starting and final configuration, a super-sonic condition locally takes place in correspondence of the root of the third vane and tip of the third rotor blade. A deeper analysis, possibly using a CFD approach, may be useful in order to exactly understand what this phenomenon is exactly connected to and may represent a natural prosecution of the present study.

Unfortunately, the target power and efficiency stated in the beginning (Table 2.6.1) could not be reached just relying on these modifications, but still a considerable power and not negligible efficiency increase may be obtained (Table 4.2.4).
As hint for future developments, there would be the possibility of analysing the blades tip clearances reduction both from a performance and from a mechanical point of view.
One additional analysis may be the re-design of the compressor blades in order to increase the compression ratio, that could be an interesting study from a theoretical point of view, but not properly from an operative point of view since the modifications on the compressor sides are very delicate and the necessity of experimentally test it emerges. Furthermore, it would be expensive and equivalent to a heavy re-design of the machine.

List of Tables

List of Figures

Reference

[1] Vaclav smil (2017) and BP Statistical Review of World Energy.

[2] "*Hydraulic and Thermal machines"*, lecture notes; D.Misul, Polytechnic of Turin.

[3] Report documents, Ethos Energy Italia S.p.A.

[4] *"Studio di fattibilità di uno scambiatore rigenerativo per impianto TG16"*, P.Capogna, Polytechnic of Turin.

[5] *"CFD Analysis of the Cooling Flow in a Heavy Industrial Gas Turbine Blade"*, F.Cardile, Polytechnic of Turin.

[6] SoftInWay. S.p.A.: User manual AxSTREAM.

[7] "Analysis of cooling solutions in a gas turbine blade by means of CHT CFD", N.Rosafio, Polytechnic of Turin.